MODELLING OF DRUG ENCAPSULATION USING VESICLES

by

Nurettin Eltuğral

B.S., in İzmir Institute of Technology, 2003

Submitted to the Institute for Graduate Studies in
Science and Engineering in partial fulfillment of
the requirements for the degree of
Master of Science

Graduate Program in Chemistry

Boğaziçi University

2006

MODELLING OF DRUG ENCAPSULATION USING VESICLES

APPROVED BY:

Prof. N. Zeynep Atay
(Thesis Supervisor) .....

Assis. Prof. Amitav Sanyal .....

Assis. Prof. Seyda Z. Bucak .....

DATE OF APPROVAL: 15/06/2006

To my family

ACKNOWLEDGMENTS

I would like to express my gratitude to my thesis supervisor Prof. N. Zeynep Atay for her continuous support, encouragement and guidance throughout this work.

I would like to thank Assoc. Prof. Seyda Z. Bucak her valuable suggestions.

I would like to thank all the members of Chemistry Department for their support and friendship.

Lastly, I would like to thank to my best friends Yavuz Fidan, İsa Değirmenci for their help, understanding and continuous support throughout my life.

Financial support for this project was provided by B.U. Research Fund (Project No: 05B503)

ABSTRACT

MODELLING OF DRUG ENCAPSULATION USING VESICLES

Aggregates of surface-active molecules consisting of one or more bilayers arranged in a hollow, closed, usually spherical geometry are termed ‘‘vesicles’’. The objective of this study was modelling of drug encapsulation using vesicles.

We have investigated the distribution of cytochrome-C protein in both SOS/CTAB and DMPC/DMPG systems at different concentrations. The results were observed spectrophotometrically. Cytochrome-C containing vesicles were isolated from the protein in the bulk by ultrafiltration of vesicle samples through 30, 100, and 300 kDa filters. Two different types of filters were used in ultrafiltration experiments. Ultrafiltration of samples was repeated for 10 times.

Ultrafiltration of SOS/CTAB containing cytochrome-C was unsuccessful because vesicle aggregation was observed during the ultrafiltration. DMPC/DMPG vesicles were also prepared with cholesterol in their bilayers. Ultrafiltration of DMPC/DMPG/protein with/without cholesterol could not be carried on with filter having polyethersulfone (PES) membrane but satisfactory results were obtained from the one with regenerated cellulose (RC) membrane.

Breakdown of DMPC/DMPG vesicles containing cytochrome-C after ultrafiltration process was done with the addition of bile salt, sodium cholate. After the breakdown, it was observed that there was no protein released, suggesting that no protein was trapped in the DMPC/DMPG vesicles without cholesterol. On the other hand, a considerable cytochrome-C signal was observed from the disintegrated DMPC/DMPG vesicles with cholesterol, suggesting that protein encapsulation was successful.

ÖZET

VESİKÜLLERLE İLAÇ KAPSÜLLENMESİNİN MODELLENMESİ

Yüzey-aktif moleküllerin oluşturduğu, bir veya daha fazla çift-katmanlı, küresel ve kapalı bir geometriye sahip olan bileşimlere "vesikül" denmektedir. Bu çalışmanın hedefi vesiküller ile ilaç kapsüllenmesinin modellenmesidir.

Değişik derişimlerdeki SOS/CTAB ve DMPC/DMPG vesiküllerinde sitokrom-C protein dağılımı incelendi. Sonuçlar UV spektrofotometresi ile gözlemlendi. Vesikül çözeltisinin 30, 100 ve 300 kDa'lık filtrelerle ultrafiltrasyonu sonucunda dışarıdaki serbest proteinlerin uzaklaştırılması sağlandı ve böylece vesiküllerin içerisinde hapsolmuş olan proteinler ayrıştırıldı. Ultrafiltirasyon işleminde iki farklı filtre kullanıldı.Vesikül örneklerinin filtrasyonu onar kez tekrarlandı.

Vesiküller kümelendiğinden, sitokrom-C içeren SOS/CTAB vesiküllerinin ultrafiltrasyonu tam olarak gerçekleştirilemedi. DMPC/DMPG vesikülleri ayrıca çift-katmanlarında kolesterol içerir halde de hazırlandı. Sitokrom-C içeren kolesterollü/kolesterolsüz DMPC/DMPG vesiküllerinin ultrafiltrasyonu polietersülfon membrana sahip olan filtrelerde başarılı sonuçlar vermedi. Ancak, aynı işlemde rejenere olmuş selüloz membrana sahip filtreler kullanıldığında memnun edici sonuçlara ulaşıldı.

Ultrafiltrasyon işleminden sonra sitokrom-C proteini içeren DMPC/DMPG vesiküllerine eklenen safra tuzu, sodyum kolayt vesiküllerin bozunmasını gerçekleştirdi. Bozunma ardından yapılan incelemelerde, çift-katmanında kolesterol bulunmayan vesiküllerin protein taşımadığı görüldü. Kolesterolle hazırlanan vesikül çözeltileri ise, bozunma sonrasında kayda değer bir protein sinyali verdiğinden, bu vesiküllerinin protein hapsetme işleminde başarılı olduğu anlaşıldı.

TABLE OF CONTENTS

ACKNOWLEDGEMENTS iv
ABSTRACT v
ÖZET vi
LIST OF FIGURES. x
LIST OF TABLES xiv
LIST OF SYMBOLS/ABBREVIATIONS xv
1. INTRODUCTION 1
2. SURFACTANTS AND SURFACTANT AGGREGATIONS 5
2.1. Surfactants 5
2.2. Self-Assembly and Packing Ratio 8
2.3. Vesicles 10
2.3.1. Types of Vesicles 10
2.3.1.1. Unilamellar Vesicles (ULV) 10
2.3.1.2. Multilamellar Vesicles (MLV) 11
2.3.1.3. Monolayer Vesicles 12
2.3.1.4. Reverse Vesicles 12
2.3.2. Surfactant Vesicles 13
2.3.3. Spontaneous Formation of Surfactant Vesicles 18
2.4. Lipids 20
2.4.1. General 20
2.4.2. Phospholipids 20
2.4.3. Lipid Vesicles 23
2.4.4. Formation Processes for Lipid Vesicles 26
2.5. Dynamics of Formation and Stability of Vesicles 28
2.6. Breakdown of Vesicles 31
2.7. Techniques in Vesicle Characterization 33
2.7.1. Cryo-TEM 34
2.7.2. QLS 35
2.7.3. DLS 36

2.7.4. Freeze-fracture Electron Microscopy 37
2.7.5. SANS 37
3. REAGENTS AND INSTRUMENTS 38
3.1. Reagents 38
3.1.1. Surfactants 38
3.1.1.1. SDS 38
3.1.1.2. SOS 38
3.1.1.3. CTAB 38
3.1.2. Phospholipids. 38
3.1.2.1. DMPC 38
3.1.2.2. DMPG 38
3.1.3. Cytochrome-C 39
3.1.4. Chloroform 39
3.1.5. Sodium Chloride (NaCl) 39
3.1.6. Sodium Hydroxide (NaOH) 39
3.1.7. Potassium dihydrogen phosphate (KH_2PO_4) 39
3.1.8. Cholesterol 39
3.1.9. Cholic Acid Sodium Salt 40
3.2. Instruments 40
3.2.1. pH-meter 40
3.2.2. Water Bath 40
3.2.3. Analytical Balance 40
3.2.4. Rotary Vacuum Evaporator 40
3.2.5. Vortex Mixer 40
3.2.6. Centrifuge 41
3.2.7. Centrifugation Filters 41
3.2.8. Extruder 41
3.2.9. Vacuum Oven 41
3.2.10. UV/VIS Spectrophotometer 42
4. EXPERIMENTAL METHODS 43
4.1. Preparation of Cytochrome-C in Distilled Water 43
4.2. Preparation of Phosphate Buffer Solution 43
4.3. Preparation of Cytochrome-C in Phosphate Buffer 43

4.4. Preparation of Sodium Cholate Solution 43
4.5. The SOS/CTAB System 43
4.5.1. Stock A 44
4.5.2. Stock B 44
4.5.3. SOS/CTAB Vesicles Containing Protein 44
4.5.4. Breakdown of SOS/CTAB Vesicles 45
4.6. The SDS/CTAB System 45
4.7. DMPC/DMPG systems 45
4.7.1. Preparation Method for Phospholipid Vesicles 45
4.7.1.1. Preparation of Lipid for Hydration 45
4.7.1.2. Hydration of Lipid Film. 45
4.7.1.3. Extrusion 46
4.7.2. DMPC/DMPG Vesicles Containing Protein 46
4.7.3. DMPC/DMPG/Cholesterol Containing Protein 46
4.7.4. Breakdown of DMPC/DMPG Vesicles 46
4.8. Ultrafiltration of Surfactant and Phospholipid Vesicles 47
4.9. Working Scheme of Ultrafiltration of DMPC/DMPG Vesicle 48
4.10. Turbidity Measurements 49
5. RESULTS AND DISCUSSION 50
5.1. SOS/CTAB Systems 50
5.1.1. General Remarks and Visual Observations 50
5.2. Breakdown of SOS/CTAB Vesicles with SOS 52
5.3. Breakdown of SOS/CTAB Vesicles with NaCl 56
5.4. DMPC/DMPG Phospholipid Vesicles. 56
5.5. Breakdown of DMPC/DMPG Vesicles 57
5.6. Ultrafiltration of Vesicles Containing Cytochrome-C 60
5.6.1. Ultrafiltration of SOS/CTAB Vesicles Containing Cytochrome-C . . . 61
5.6.2. Ultrafiltration of DMPC/DMPG Vesicles Containing Cytochrome-C . 61
6. CONCLUSION 67
7. SUGGESTIONS FOR FURTHER WORK 69
8. REFERENCES 70

LIST OF FIGURES

Figure 1.1. Preparation of protein-encapsulating vesicles 2

Figure 1.2. Release of the "encapsulated" protein upon breaking down of the vesicles 3

Figure 1.3. "Ideal" drug delivery system 4

Figure 2.1. Schematic representation of a surfactant molecule 5

Figure 2.2. Open structure of anionic surfactant, SOS 6

Figure 2.3. Open structure of cationic surfactant, CTAB 6

Figure 2.4. Open structure of DMPC 6

Figure 2.5. Space-filling model of DMPC 7

Figure 2.6. Open structure of DMPG 7

Figure 2.7. Space-filling model of DMPG 7

Figure 2.8. Orientation of surfactant molecules in aqueous media 8

Figure 2.9. A schematic drawing of a surfactant molecule, showing the curvature packing parameter 9

Figure 2.10. A schematic drawing of surfactant aggregates 9

Figure 2.11. An ULV structure 11

Figure 2.12. A schematic representation of MLV 11

Figure 2.13. Schematic representation of monolayer vesicle 12

Figure 2.14. A schematic representation of reverse vesicle 13

Figure 2.15. Chemical structure of the fluorescence probe prodan 14

Figure 2.16. Microstructures formed at room temperature for the ternary system of CTAB/SOS/H_2O. On the equimolar line, a 1:1 crystalline precipitate forms 15

Figure 2.17. A schematic phase diagram of a mixture of a cationic and an anionic surfactant 19

Figure 2.18. Components of phospholipids 21

Figure 2.19. (a) Schematic diagram of a phospholipid molecule (b) structure of phosphatidylcholine (lecithin) 22

Figure 2.20. Types of phospholipids 23

Figure 2.21. Aggregation of phospholipid in water 24

Figure 2.22. Formation of vesicle from phospholipid bilayer 27

Figure 2.23. A schematic representation of pathways that may be involved in the transition form micelles to unilamellar vesicles 29

Figure 2.24. Schematic of the intermediate states that may be involved during the formation and growth of vesicles in SOS/CTAB system 30

Figure 2.25. Ternary phase diagram for CTAB/SOS/H_2O at 25 ^{0}C 32

Figure 2.26 (a) Electron micrograph of thin section of phospholipid vesicles; (b) diagram of vesicle in cross section 33

Figure 2.27 Cryo-TEM image of CTAB/SOS/H_2O 34

Figure 2.28 Cryo-TEM image of CTAT/SDBS vesicles 35

Figure 2.29 Freeze-fracture electron micrograph of MLV in TDMAO/TTABr/hexanol system 37

Figure 5.1. Phase diagram of SOS /CTABH_2O ternary systems 51

Figure 5.2. Absorbance data for Stocks II, III, IV, and V as a function of time . . . 52

Figure 5.3. Absorbance of Stock II at 300 nm as a function of added Stock B, and distilled water 53

Figure 5.4. Absorbance versus wavelength plot of Stock II containing 0.2 mg/mL cytochrome-C 53

Figure 5.5. Absorbance versus wavelength plot of Stock II containing 0.11 mg/mL cytochrome-C after addition of 1.5 mL Stock B 54

Figure 5.6. Absorbance of Stock II at 300 nm containing cytochrome-C as a function of added Stock B, and distilled water 54

Figure 5.7. Absorbance of 2 mL Stock II containing cytochrome-C at 300 nm as a function of added NaCl, and distilled water 56

Figure 5.8. Absorbance at 300 nm for 1 mL S1 as a function of added 0.1 M sodium cholate, and phosphate buffer 58

Figure 5.9. Absorbance at 300 nm for 1 mL S2 as a function of added 0.1 M sodium cholate, and phosphate buffer 58

Figure 5.10. Absorbance for cytochrome-C at 408 nm in S1 as a function of added 0.1 M sodium cholate, and phosphate buffer 59

Figure 5.11. Absorbance of cytochrome-C at 408 nm for filtrates of S3 62

Figure5.12. Absorbance versus wavelength plot of Filtrates of S3 63

Figure 5.13. Absorbance versus wavelength plot of S3 after ultrafiltration 63

Figure 5.14. Absorbance of cytochrome-C measured at 408 nm wavelength for filtrates of S1 64

Figure 5.15. Absorbance versus wavelength plot of Filtrates of S1 65

Figure 5.16. Absorbance wavelength plot of encapsulated cytochrome-C 66

LIST OF TABLES

Table 2.1. Aqueous systems reported to form vesicles spontaneously 17

Table 2.2. QLS results for mixtures of CTAB and SOS, measured immediately following 36

Table 3.1. Parameters for UV/VIS spectrometer 42

Table 5.1. Amount of SOS and CTAB in stock solutions 50

Table 5.2. pH analysis of stocks 51

Table 5.3. Absorbance change of cytochrome-C upon vesicle breakdown 55

Table 5.4. Compositions of phospholipid vesicles. 57

Table 5.5. Technical specifications of ultrafiltration devices 60

LIST OF SYMBOLS /ABBREVIATIONS

a_s	Surfactant head group area
L	Lamellar phase
l_s	Surfactant optimum chain length
M	Spherical micelle
P	Packing parameter
R	Rode-like micelle
T_C	Phase transition temperature
V	Unilamellar anionic-rich vesicles
V_c	Unilamellar cationic-rich vesicles
V_s	Hydrophobic volume

ABS	Absorbance
ADP	Adenozine 5-diphosphate
AOT	Bis-2-ethylhexylsulfosuccinate
CMC	Critical micelle concentration
Cryo-TEM	Cryogenic transmission electron microscopy
CTAB	Cetyltrimethylammonium bromide
CTAT	Cetyltrimethylammonium tosylate
DDAB	Didocecyldimethylammonium bromide
DLS	Dynamic light scattering
DMPC	1,2-Dimyristoyl-sn-Glycero-3-Phosphocholine
DMPG	1,2-Dimyristoyl-sn-Glycero-3-[Phosphorac-(1-glycerol)]-sodium salt
GUV	Giant unilamellar vesicles
KH_2PO_4	Potassium dihydrogen phosphate
LUV	Large unilamellar vesicles
LUVETs	Large unilamellar vesicles by extrusion techniques
MLV	Multilamellar vesicles
MWCO	Molecular weight cut off
NaBr	Sodium bromde

NaCl	Sodium Chloride
NaOH	Sodium hydroxide
OG	Octyl glucoside
PES	Polyethersulfone
POPC	1-palmitoyl-2-oleoyl-sn-glycero-3-phosphocholine
PVP	Polyvinylpyrrolidone
QLS	Quasi-elastic light scattering
RC	Regenerated cellulose
SANS	Small-angle neutron scattering
SDBS	Sodium dodecyl benzyl sulfonate
SDS	Sodium dodecyl sulfate
SOS	Sodium octyl sulfate
SUV	Small unilamellar vesicles
TDMAO	Tetradecyldimethyamine oxide
TTABr	Tetradecyltrimethylammonium bromide
ULV	Unilamellar vesicles
Wt	Weight

1. INTRODUCTION

It is well known that in aqueous solutions, amphiphilic molecules such as synthetic surfactants and natural phospholipids arrange into a bilayer conformation, wherein the hydrophilic polar head groups orient toward the center where they are shielded from the aqueous environments [1].

Vesicles are broadly defined as bilayers of surfactants or lipids surrounding an aqueous space. In 1965, Bangham *et al.* showed that phospholipids dispersed in water formed vesicles capable of separating an internal compartment from the bulk solution. As a result, they have become the preferred structure in most applications. These vesicles are now being used as biomimetic synthetic membranes. During 1970s, there has been great increase of interest in the application of lipid vesicles for delivery of drugs [2].

Kaler *et al.* observed spontaneous formation of vesicles by mixing aqueous solutions of cationic and anionic surfactants. These mixtures of oppositely charged surfactants exhibit many features similar to those observed in biological mixtures and, therefore, are convenient model systems for the investigation of phase behavior and morphology. If the biocompatibility can be further improved, surfactant vesicles will substitute the lipid vesicles sooner or later. However, the insufficient stability of these self-assembled structures is still a major problem. This may limit their practical applications [3].

Drug delivery systems have been attracting a lot of attention in the recent years. However, many of the suggested systems have limited applications in vivo. In order to design a stable, biologically compatible, completely inert and body-harmless drug-carrier requires that the carrier should be surface modified so that it recognizes the target site and binds to the target, and the drug should be released at the site.

The aim of this work is to mimic a carrier system where “drug” will be encapsulated by the vesicles, and then released by breaking down these vesicles. In this

study, modelling of a drug encapsulation system is done using vesicles prepared from both synthetic and natural surfactants.

The initial work involves the entrapment of a coloured protein, cytochrome-C, in vesicles prepared from synthetic surfactants sodium octyl sulfate (SOS) and cetyltrimethylammonium bromide (CTAB). All free cytochrome-C outside the vesicles are discarded by ultrafiltration (Figure 1.1). These SOS/CTAB vesicles can then release the protein upon breaking up of the vesicles with salt or one of the surfactants (Figure 1.2). The vesicles containing cytochrome-C in the aqueous core can be visualised as a model for phospholipid vesicles encapsulating "drugs" and these are extremely important in target drug delivery systems. Since cytochrome-C gives absorbance at 408 nm, the distribution of the protein can be observed spectrophotometrically.

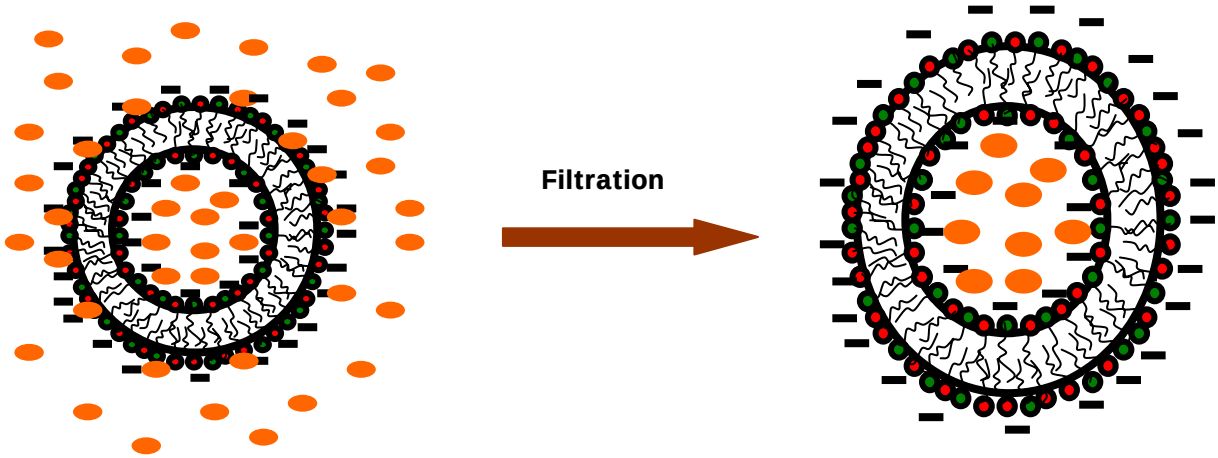


Figure 1.1. Preparation of protein-encapsulating vesicles

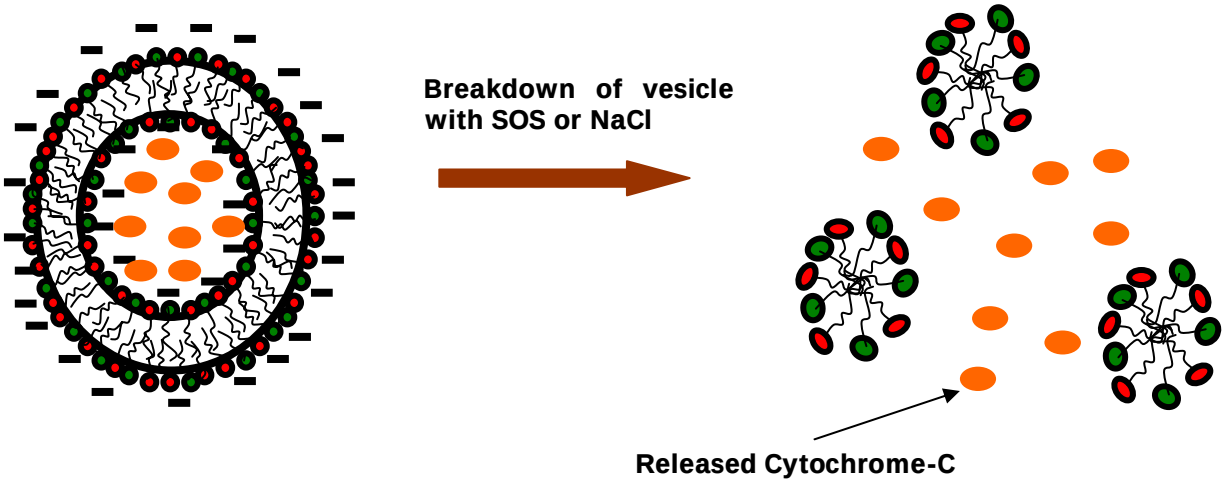


Figure 1.2. Release of the "encapsulated" protein upon breaking down of the vesicles

The next step is to change the nature of the vesicle, from synthetic surfactants SOS and CTAB, to biocompatible ones where the bilayer is made up of phospholipids 1,2-Dimyristoyl-sn-Glycero-3-Phosphocholine (DMPC) and 1,2-Dimyristoyl-sn-Glycero-3-[Phophorac-(1-glycerol)]-sodium salt (DMPG). These vesicles can also be broken down with salt and the release of the protein is observed.

The ultimate aim is to design a suitable "drug delivery system", in which a useful "drug" is encapsulated and "target deliver" this drug to a "deformed" site where it should be released (Figure 1.3). In an ideal system, the vesicle bilayer peptide amphiphiles (e.g. interleukin-8, IL-8) can be integrated to recognize a macrophage inflammatory protein such as chemokine which is released only at the site of inflammation or infection. After the binding of liposomes to the site, a solution of bile salt (such as cholate) can be injected to the blood stream. Cholate is a micelle forming bile salt and mixes well with phospholipids. At a certain ratio of phospholipid to cholate, liposomes will disintegrate to form mixed micelles and therefore release the drug. In order to target cholate micelles in the blood stream to the same location, chemokine receptor can also be integrated in the inner core of micellar cholate.

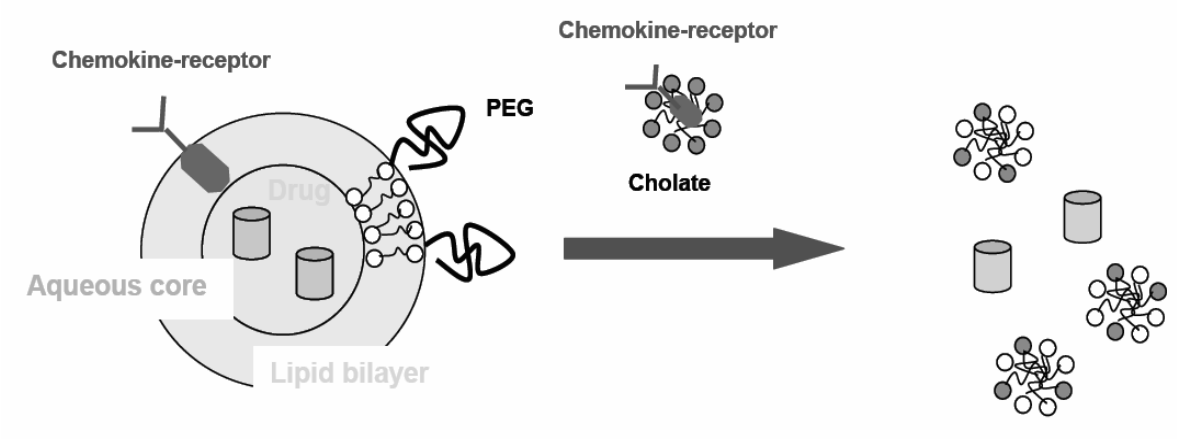


Figure 1.3. “Ideal” drug delivery system

Our intention is to design a biomimetic system under laboratory conditions and then to extent it to the “ideal system” described above.

2. SURFACTANTS AND SURFACTANT AGGREGATIONS

2.1. Surfactants

Substances that accumulate at water surfaces and change the surface properties are called surface-active-agents (surfactants). Surfactants, also known as wetting agents, detergents, emulsifiers, are amphiphilic molecules that are composed of a hydrophobic tail and a hydrophilic head group. Therefore, they are sparingly soluble in both organic solvents and water.

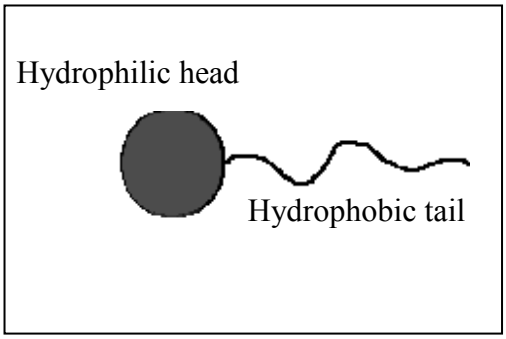


Figure 2.1.Schematic representation of a surfactant molecule

A surfactant can be classified by the electrical charge in its head group. A nonionic surfactant has no charge, whereas, the head group of an ionic surfactant carries a net charge. If the charge is negative, the surfactant is called anionic; if the charge is positive, it is called cationic. If a surfactant head contains two oppositely charged groups, it is termed zwitterionic. Another classification of surfactants is synthetic and natural surfactants. The anionic surfactant, SOS and a cationic surfactant, CTAB can be given as examples to synthetic surfactants [4].

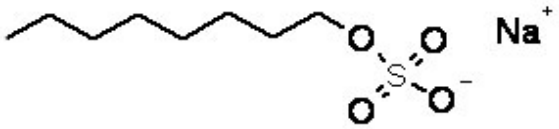


Figure 2.2.Open structure of anionic surfactant, SOS

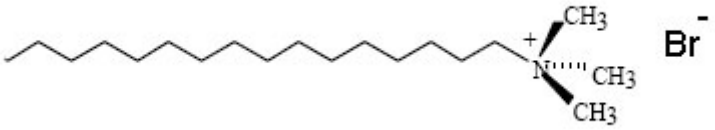


Figure 2.3.Open structure of cationic surfactant, CTAB

Phospholipids are one of the types of naturally occurring surfactants with two hydrophobic tails. The neutral lipid, DMPC and a negatively charged lipid, DMPG are two examples to naturally occurring surfactants [5].

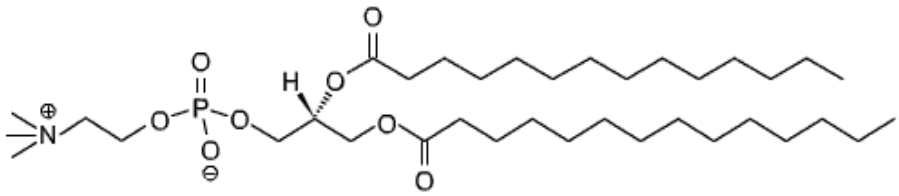


Figure 2.4. Open structure of DMPC

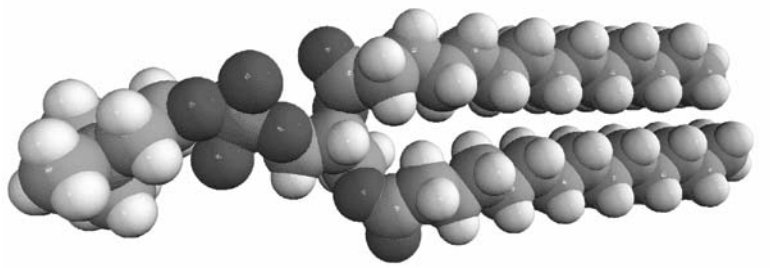


Figure 2.5. Space-filling model of DMPC

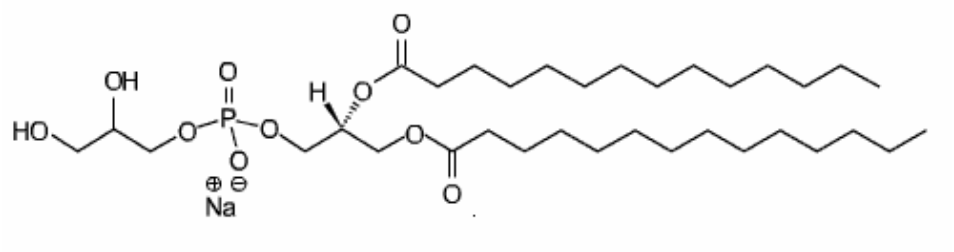


Figure 2.6. Open structure of DMPG

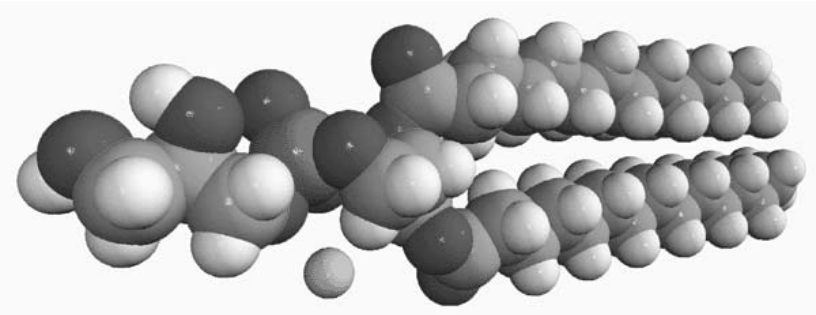


Figure 2.7. Space-filling model of DMPG

2.2. Self-Assembly and Packing Ratio

Amphiphilic molecules, due to their dual character (hydrophobic tail and hydrophilic head group) and the electrostatic interactions, self-assemble in aqueous solutions in a variety of morphologically surfactant aggregate structures [6].

Micelles are the simplest form of self-assembled structures. In these structures, the molecules are arranged with tails in the center and the head groups around the surface. Micelles only form when the concentration of surfactant is greater than the critical micelle concentration (CMC). The driving force for this aggregation process is the hydrophobic tail groups that are largely able to avoid the unfavorable surface energies associated contacting the water molecules.



Figure 2.8.Orientation of surfactant molecules in aqueous media

A variety of different shapes are observed that range from spherical and rod-like micelles to amphiphilic bilayer. A bilayer is a planar sheet of two layers of molecules arranged with the tails in the middle and the head groups on the surface.

The actual form assumed by an aggregate depends on the molecular constituents of the amphiphilic and can be explained by simple geometric consideration. The geometry of an amphiphile is described by the packing parameter *P* of the amphiphile, which is defined as the ratio of the hydrophobic volume (V_s) to the product of the head group area (a_s) and optimum chain length (l_s) [7].

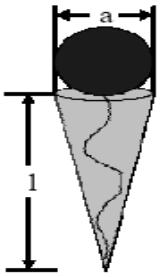


Figure 2.9. A schematic drawing of a surfactant molecule, showing the curvature packing parameter

$$P = \frac{V_S}{(a_S \times I_S)} \tag{2.1}$$

The packing parameters then determine which structure will form. In forming space filling aggregates, for $P < 1/3$ spherical objects, for $1/3 < P < ½$ rod-like particles, and for $½ < P$ bilayer structures are expected, while for values of p larger than 2, reverse structures should be formed.

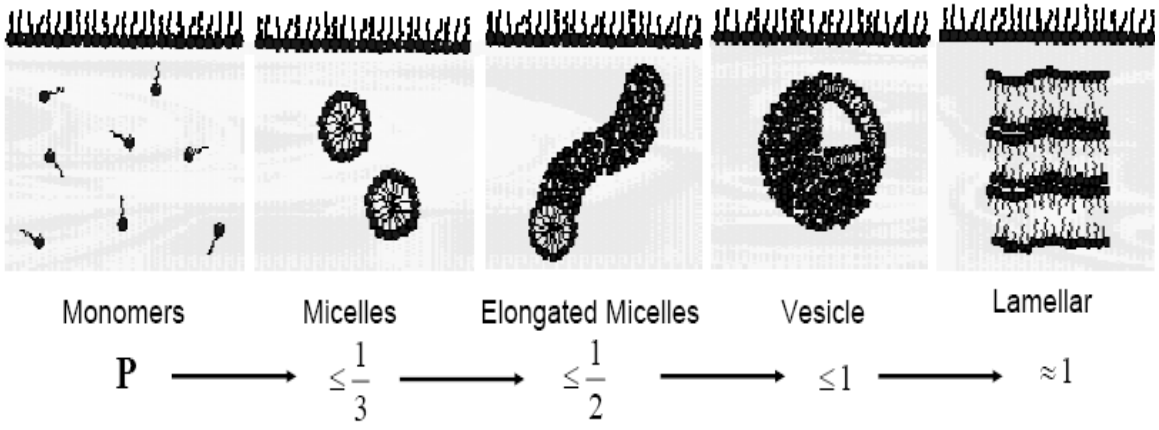


Figure 2.10. A schematic drawing of surfactant aggregates

2.3. Vesicles

In general, packing parameters work well for the explanation of experimentally observed amphiphilic structures. As mentioned above, one very common method of self-assembly is the formation of amphiphilic bilayers. When a bilayer curves into a spherical structure it is called a vesicle [7]. In the other words, vesicles are closed bilayers of surfactants or lipids. They are used as delivery vehicles for drugs, enzymes, antibodies, and genetic material. They are also considered as micro-reactors in nanoparticle synthesis [1, 5-10].

2.3.1. Types of Vesicles

Vesicles are classified as follows:

2.3.1.1. Unilamellar Vesicles (ULV). These are vesicles with one single bilayer around the inner aqueous compartment. Here one can distinguish between small unilamellar vesicles, SUV with diameter = 20-100 nm, large unilamellar vesicles, LUV with diameter = 100 nm- 1 μm, and giant unilamellar vesicles, GUV with diameter = 1-50 μm [1, 8].

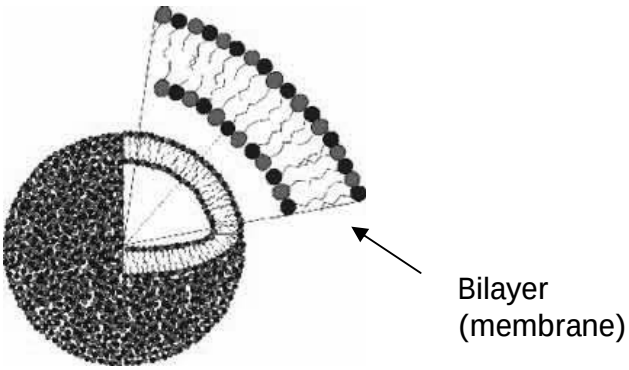


Figure 2.11. An ULV structure

2.3.1.2. Multilamellar Vesicles (MLV). These are vesicles with more than one bilayer where one has additional bilayers added to the surface analogous to the many layers of skin on an onion [1, 7]. Aggregate structures such as spherical and rod-like micelles, vesicles, lamellar phases, and precipitates have all been observed depending on the concentrations of the two surfactants in the solutions. As a general tendency, one finds that ULV are more likely to be observed for dilute systems, while MLV are frequently found in more concentrated surfactant systems.

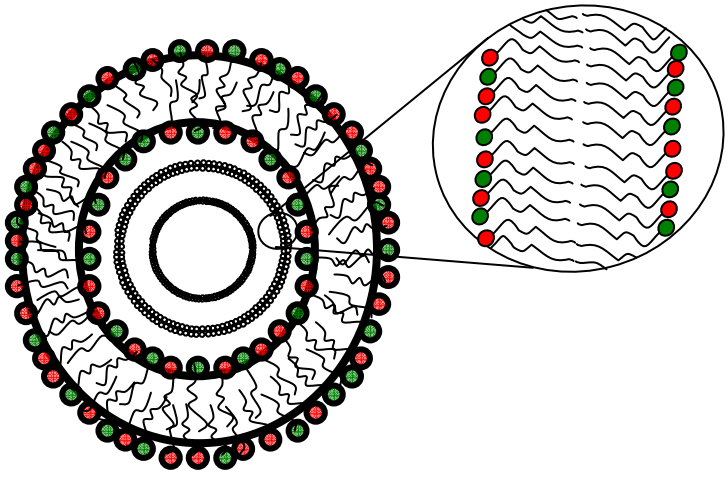


Figure 2.12. A schematic representation of MLV

Typically, for bilayer-forming amphiphilic systems, one observes that with increasing concentration there exists a structural progression according to

ULV → MLV → planar bilayers

2.3.1.3. Monolayer Vesicles. These are vesicles with hydrophilic head groups at both ends of the hydrophobic chains. The resulting membrane consists of a single molecular layer.

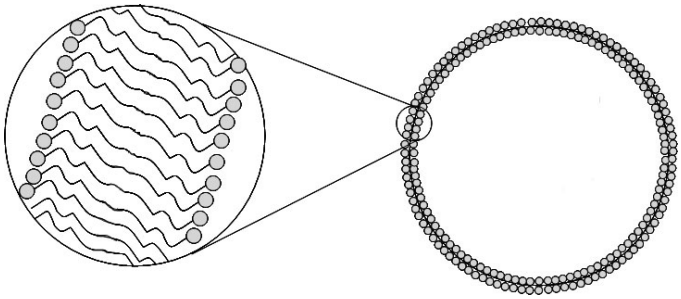


Figure 2.13. Schematic representation of monolayer vesicle

2.3.1.4. Reverse Vesicles. These are vesicles whose inner compartment and the outer compartment media are apolar solvents [11].

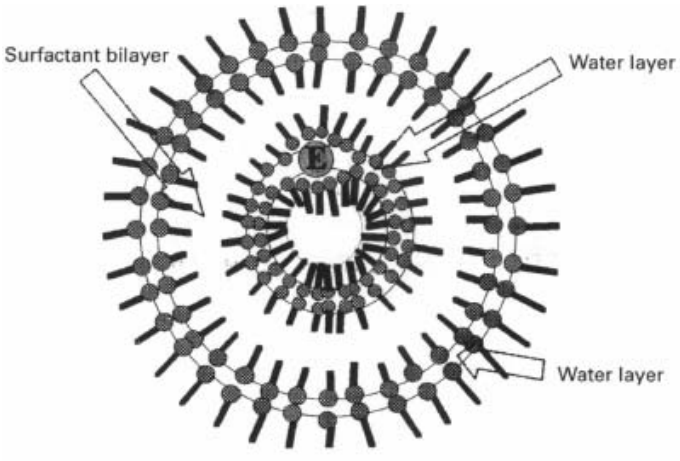


Figure 2.14. A schematic representation of reverse vesicle

2.3.2. Surfactant Vesicles

Aqueous mixtures of oppositely charged surfactants exhibit interesting phase behavior and properties. It is found that structures similar to those formed in biological phospholipid systems form in mixtures of oppositely charged synthetic surfactants. Vesicles form spontaneously when oppositely charged surfactants are mixed in aqueous solution. It is important to know how the solution composition and molecular geometry of the surfactants influence the resulting microstructure and phase behavior. Both in biological systems and synthetic surfactant mixtures, strong growth of long (several micrometers) rode-like micelles occur between vesicular and micellar phases. The size, surface charge, permeability of the bilayer in surfactant vesicles can be adjusted through the varying the chain length and the relative amount of the two surfactants [6]. Thus, mixtures of oppositely charged synthetic surfactants can be used as models of biological systems to identify the relationship between solution conditions and the resulting microstructures [2].

Formation of vesicles from synthetic amphiphiles was first reported by Kunitake and Okahata [12] in 1977, just by dispersing didodecyldimethylammonium bromide (DDAB) in water followed by sonication.

There is a vast literature describing the course of vesicle systems in synthetic surfactant mixtures. Yatcilla *et al.* [3] have investigated phase behavior and aggregate

morphology of mixtures of oppositely charged surfactants CTAB and SOS with cryogenic transmission electron microscopy (cryo-TEM) and quasielastic light scattering (QLS). It is shown that vesicles form spontaneously when CTAB and SOS are mixed in aqueous solution. The chain length asymmetry appears to stabilize vesicles relative to other microstructures. Bilayer properties are also determined by the composition. Vesicles prepared with an excess of long tailed surfactant have bilayers stiffer than those rich in the short tailed surfactant.

An extensive fluorescence spectroscopy study was done by Karukstis *et al.* [13] for the cationic/anionic (CTAB/SOS), hence, the shortened term ‘‘catanionic’’ surfactant systems in the dilute surfactant region. The polarity-sensitive fluorophore prodan can be used to mark off the boundaries of the surfactant microstructures of the ternary system of CTAB/SOS/H_2O.

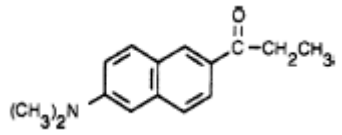


Figure 2.15. Chemical structure of the fluorescence probe prodan

In the dilute surfactant region of the CTAB/SOS/H_2O system up to nine solution-phase aggregate regions occur at fixed total surfactant concentration, including aggregates of CTAB-rich rode-like micelles (R), and cationic-rich unilamellar vesicles ($R+V_c$), unilamellar cationic-rich vesicles (V_c), anionic-rich unilamellar vesicles and a lamellar phase (V+L), unilamellar anionic-rich vesicles (V), rode-like SOS-rich micelles and unilamellar anionic-rich vesicles (R+V), SOS-rich rodlike micelles (R), and spherical SOS-rich micelles (M).

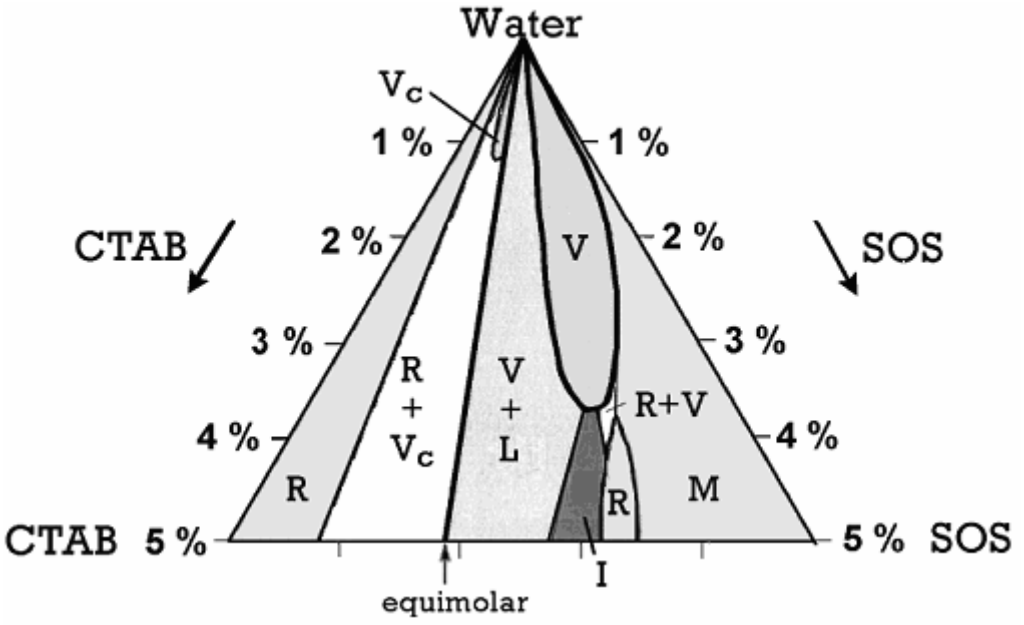


Figure 2.16. Microstructures formed at room temperature for the ternary system of CTAB/SOS/H_2O. On the equimolar line, a 1:1 crystalline precipitate forms [13]

This study demonstrates that a fluorescence spectroscopic approach using the probe prodan is a sensitive and efficient technique to mark off the boundaries of aggregate regions in surfactant systems. This spectroscopic method is a promising approach to assist in understanding the principles governing aggregate formation in complex surfactant systems.

Almgren and co-workers investigated mixtures of CTAB and SOS with the latter in excess over a long time, about 500 days. They followed the growth of aggregates by dynamic light scattering (DLS) and checked the morphologies by cryo-TEM. The results show that the spontaneous vesicle populations do not represents equilibrium populations. The vesicles and the open structures form spontaneously as a result of interfacial charge but are not at equilibrium. Marques made a through study of spontaneous cationic vesicles. He claimed to show that these vesicles are equilibrium structures, but the fact is that his study proves that they are not [14].

The incorporation of peptides and oligopeptides into the hydrophilic domains of amphiphiles has led to new classes of surfactants that self-assemble into structures that mimic a variety of functions of natural materials. Luk and Abbott [15] focused on

advances in the applications of amphiphiles that depend on the development of highly functional molecules in four categories: (1) peptide-functionalized amphiphiles, (2) carbohydrate-functionalized amphiphiles, (3) redox-active amphiphiles and (4) polymerizable amphiphiles. The design of redox-active and polymerizable surfactants offers interesting possibilities for applications at the interface of disciplines of biology, engineering and chemistry.

Zhai *et al.* [6] investigated the interaction between the mixture of sodium dodecyl benzyl sulfonate (SDBS)/CTAB and polymer by using a fluorescence method, pyrene as a probe. The polarity change of pyrene environment is accompanied with the change which reflects the relative position of the polymer and vesicle/micelle. Since polyvinylpyrrolidone (PVP) tends to be positive in solution, an interaction was observed between PVP and anionic micelle or anionic surfactant-rich vesicle, based on analysis on the polarity in the fluorescence spectrum of pyrene. But there is no interaction between PVP and cationic micelle or cationic surfactant-rich vesicle. The micelle adheres to PVP, but PVP insert into bilayer of vesicle. The electrostatic attraction is essential in the interaction between polymer and surfactant association structure.

The various surfactants that have been reported to form vesicles spontaneously have been reviewed by Kaler *et al.* [2] and are summarized in Table 2.1.

Table 2.1. Aqueous systems reported to form vesicles spontaneously [2]

Type	**System**
Mixture of soluble cationic and anionic surfactants	C_8 to C_{16} alkyltrimethylammonium tosylates or bromides + SDBS (commercial), C_8 to C_{12} alkyl sulfates or benzene sulfonate
Mixture of soluble cationic and anionic surfactants	Alkyltrimethylammonium alkanoates
Mixture of soluble and insoluble cationic surfactants	Mixed alkyltrimethylammonium hydroxides (or acetates) and bromides
Mixture of soluble and insoluble anionic surfactants	Mixed sodium and choline salts of AOT (bis-2-ethylhexyl sulfosuccinate)
Soluble surfactant + amphiphilic oil	Soap-fatty acid mixtures
Soluble surfactant + amphiphilic oil	Lysolecithin-fatty acid mixtures
Soluble surfactant + amphiphilic oil	Soap-fatty alcohol mxtures
Soluble surfactant + amphiphilic oil	Soap-cholesterol mixtures

2.3.3. Spontaneous Formation of Surfactant Vesicles

Within the last decade, a theoretical concept together with important new experimental observations have suggested that vesicles may form ‘‘spontaneously’’, and may even constitute an ‘‘equilibrium’’ state. While the formation of vesicle may indeed occur spontaneously, it is highly improbable that mixtures having vesicular (hollow spherical) structures ever constitute the true equilibrium state [16].

The word ‘spontaneous’ is defined in the 1986 Webster’s Third New International Dictionary as caused by internal energy, controlled and directed internally, or developing without apparent external influence of force [16]. Spontaneous formation of vesicles is an important process because here no such external force is required. One early observation of spontaneous vesicle formation is in the case of dialkyl dimethylammonium hydroxide surfactants. The surfactant molecules do not form planer bilayers but have a tendency to form curved bilayers such as vesicles. Another case of spontaneous vesicle formation is observed in the mixture of anionic carboxylate surfactant with the corresponding acid as a co-surfactant as a function of pH [7].

Meanwhile, a classical situation for spontaneous formation of vesicles is the mixture of a cationic and an anionic surfactant, with either one in excess. It was noted that vesicles for mixtures of CTAB and sodium dodecyl sulfate (SDS) form spontaneously. Kaler *et al.* [2] demonstrated the existence of spontaneous monodisperse equilibrium vesicles in aqueous mixtures of cetyltrimethylammonium tosylate (CTAT) and SDBS. Vesicles also form spontaneously over a wide range of compositions in SOS and CTAB solutions [3].

For equimolar composition of anionic surfactant and cationic surfactant mixture, precipitation may take place while unilamellar vesicles are formed. In the phase diagram in Figure 2.17 transitions have been observed in system CTAB/SOS, depending on the total concentration of amphiphile [7]. Tendency for precipitation increases with the length of the alkyl chains and also similar chain lengths of the amphiphiles will cause precipitation; therefore large differences in chain length are preferred.

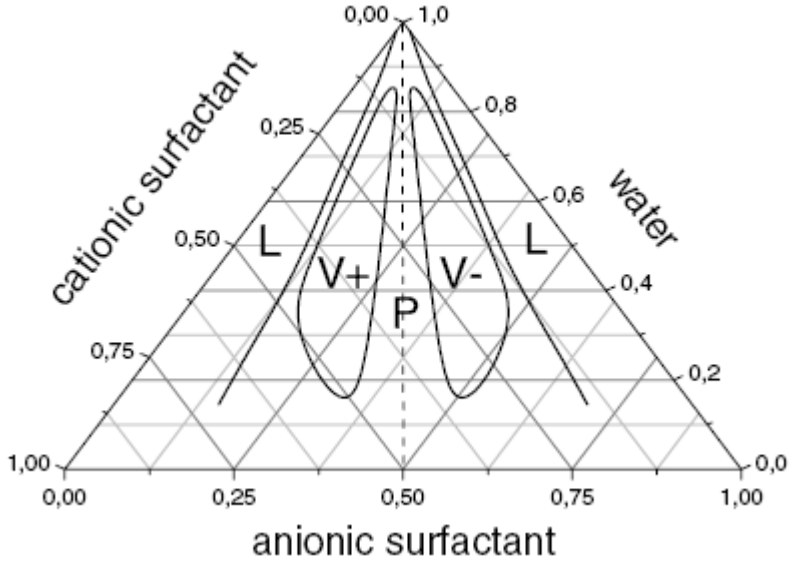


Figure 2.17. A schematic phase diagram of a mixture of a cationic and an anionic surfactant [7]

It should be noted that mixing of anionic and cationic surfactants leads not only to the formation of a cationic-anionic surfactant pair but also to an equal amount of salt being formed by the corresponding counter ions and this means that such systems have a considerable ionic strength. However, it is also possible to have such systems without additional salts. This can be achieved by mixing the acid of the anionic surfactant with the hydroxide of the corresponding cationic surfactant to yield water. Such salt free vesicle systems exhibit larger vesicle region in the phase diagram [7].

Finally, it should be stated that there are other situations where spontaneous vesicle formation has been observed.

2.4. Lipids

2.4.1. General

The lipids are a large and diverse group of naturally occurring compounds that are related by their solubility in nonpolar organic solvents (e.g. ether, chloroform, acetone, and benzene) and general insolubility in water. Lipids play an important role in cell structure and function. Biological membranes are organized assemblies of lipids and proteins. There are different types of lipids which have diverse structural properties [17]. Basic structures of lipids are as follows:

- Triacylglycerides
- Phospholipids
- Plasmalogens
- Sphingolipids

In this section, mainly the structures and physical properties of phospholipids are discussed.

2.4.2. Phospholipids

Phospholipids are the main constituents of cell membranes. They are formed from glycerol, two fatty acids, and a phosphate group with some other molecule attached to its other end. The hydrocarbon tails of the fatty acids are still hydrophobic, but the phosphate group end of the molecule is hydrophilic because of the oxygens with all of their pairs of unshared electrons. This means that phospholipids are soluble in both water and oil.

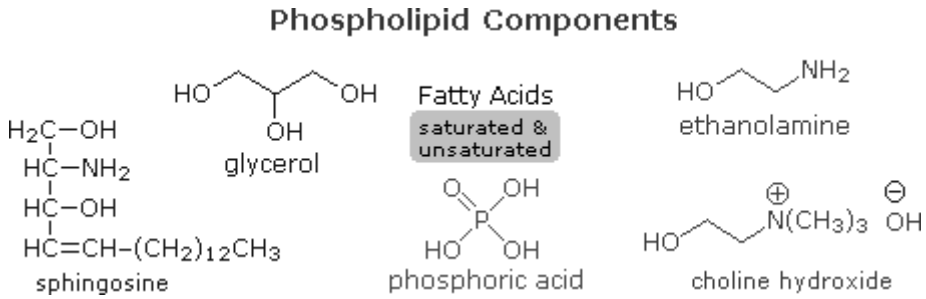


Figure 2.18. Components of phospholipids

The building block of the phospholipids is phosphatidic acid which results when hydrogen substituted to the other end of the phosphate group. Substitutions include ethanolamine (phosphatidylethanolamine), choline (phosphatidylcholine, also called lecithins), and serine (phosphatidylserine) [18].

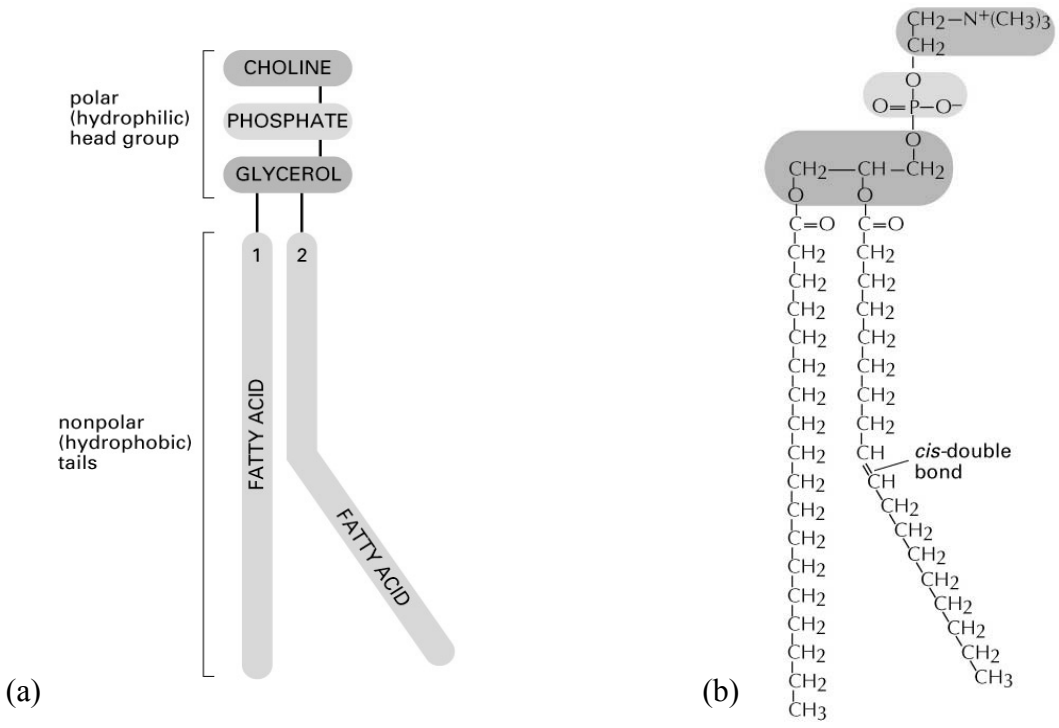


Figure 2.19. (a) Schematic diagram of a phospholipid molecule (b) structure of phosphatidylcholine (lecithin)

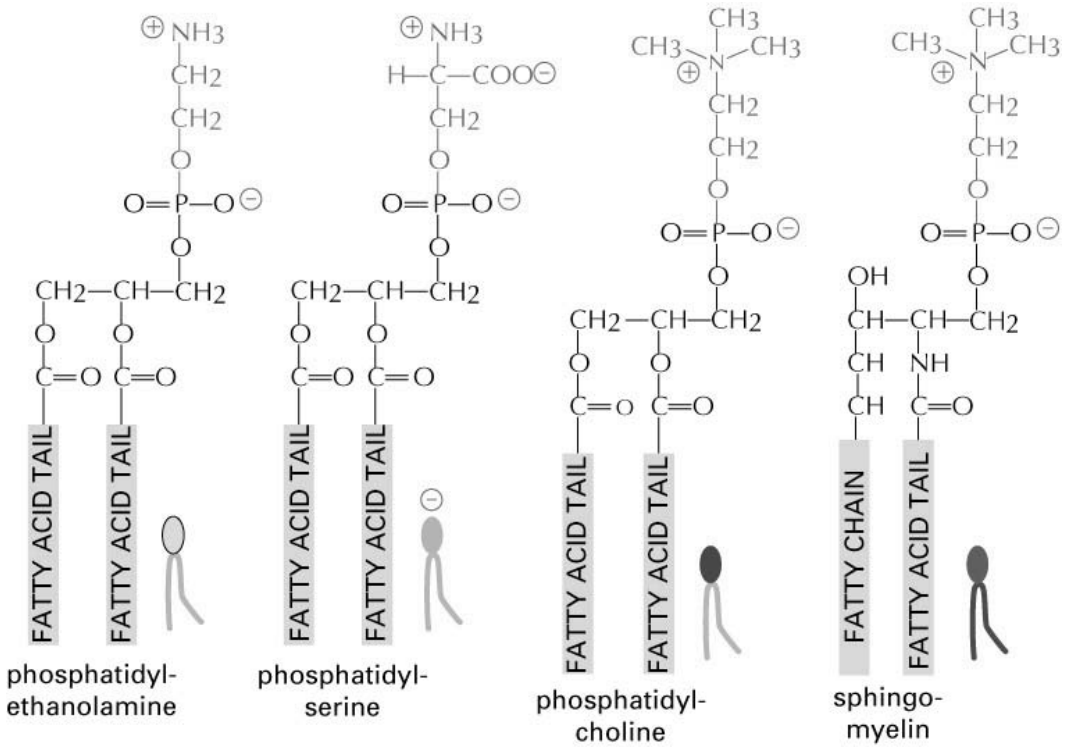


Figure 2.20. Types of phospholipids

As ionic amphiphiles, phospholipids aggregate or self-assemble when mixed with water. The alkyl chains present in phospholipids and the mixed charges in their head groups, micelle formation is unfavorable relative to bilayer structure. They orient in a different manner than the soaps and detergents. Bilayer structure is created when phospholipids dispersed in water, upon application of external energy. As shown in the following diagram the polar head groups are on the faces of the bilayer contacting with water, and the hydrophobic alkyl chains form a nonpolar interior [18].

2.4.3. Lipid Vesicles

Lipid vesicles (also known as liposomes in biology) are microscopic polymolecular aggregates that are spherical. They are formed when phospholipids are vigorously mixed with water. Unlike micelles, lipid vesicles have both aqueous interiors and exteriors.

Vesicles composed of phospholipids have been extensively studied as models for biological membranes. The stability of liposomes and their impermeability to many

substances makes them promising vehicles for the delivery of therapeutic agents, such as drugs and enzymes, to particular tissues [9]. If methods can be developed for targeting phospholipid vesicles to specific cell populations, then drugs could be directed towards particular tissues through vesicle encapsulation [17].

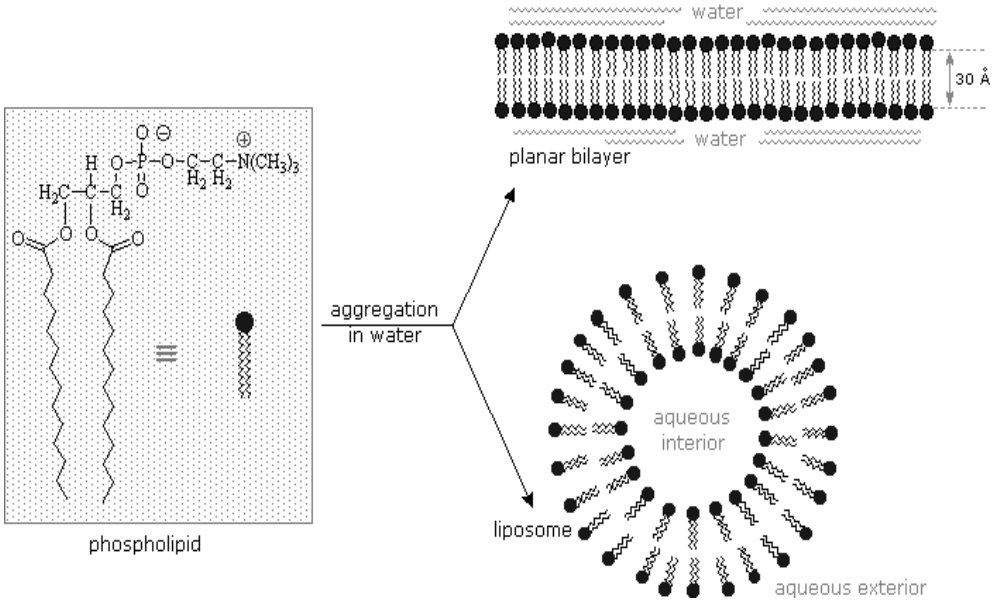


Figure 2.21. Aggregation of phospholipid in water

In 1965 Bangham discovered that the particles which exist within dilute aqueous mixtures of polar lipids have a roughly spherical shape and enclose part of the liquid phase [19]. From their size it was evident that these particles were aggregates of many molecules, and from other information it was apparent that the molecules within each layer were arranged in bilayers.

Permeability properties of lipids play a key role when lipid vesicles are used as nano- or micrometer-sized reaction compartments. Sometimes, the bilayer permeability can be modified by the addition of bilayer-soluble molecules. Surfactants show affinity for lipid bilayers without destroying them, as long as the surfactant concentration is not higher than the lowest concentration for bilayer solubilization. Treyer *et al.* [8] focused on the uptake of nucleotides by phospholipid vesicles at low solubilizing cholate concentrations in equilibrated systems. The uptake experiments were preceded by the interaction between cholate and 1-palmitoyl-2-oleoyl-sn-glycero-3-phosphocholine (POPC). Nucleotide uptake

by the vesicles at the solubilizing cholate concentration was confirmed in the case of adenozine 5-diphosphate (ADP) by using vesicles containing entrapped *Micrococcus luteus* polynucleotide phosphorylase, which catalyzed the endovesicular polymerization of exovesicularly added ADP. The results show that enzyme-coating vesicles can be used as nanoreactor systems in which the permeability of the bilayers is selectively altered by a surfactant, allowing the uptake of substrate molecules but not the release of the entrapped enzyme or reaction product.

Helenius and Simons [20] have described the addition of increased amounts of detergent to phospholipid vesicles as occurring in three stages: (1) the detergent is incorporated into the bilayer and causes changes in its physical properties, (2) saturation of the bilayer with detergent followed by vesicle to mixed micelle transition, (3) size of the mixed micelles decreases as the detergent/phospholipid ratio is increased.

Jackson *et al.* [21] have studied the solubilization of egg phosphatidyl choline vesicles by the nonionic detergent octyl glucoside (OG). A sharp increase in turbidity followed by rapid clearing is reported during titration of the vesicles with OG. The turbidity peak occurs at the point when the vesicles are saturated with detergent. During the drop in turbidity following the maximum, the detergent to lipid ratio in the vesicles remains constant as the vesicles are solubilized into mixed micelles. Jackson concludes that the turbidity increase is a result of vesicle fusion.

Binford and Wadso [22] studied the enthalpy and solubilization of DMPC which is a neutral (noncharged) lipid. Cholate, deoxycholate, and lithocholate added to DMPC at 20^{o}C. Flow calorimetry is used to determine the enthalpy change resulting from the addition of sodium cholate to DMPC vesicles. For the addition of detergent to vesicles the difference between enthalpy measurements above and below the transition temperature gives an indication of bilayer disruption.

Goldmann *et al.* [5] have determined the molar affinity of talin and vinculin to charged phospholipid DMPC/DMPG, which is negatively charged vesicles by light scattering. Light scattering technique can be used as an effective tool for the study of

temperature-dependent protein-lipid interactions/insertions. Talin and vinculin are inserted into the hydrophobic core of lipid membranes.

Experimental approaches are described on vesicle systems which host a chemical reaction within the bilayer boundary of the vesicles; chemical reaction coverts substrate molecules into the components of the boundary leading an increase of the boundary interphase and eventually to a reproduction of the vesicles. Since reproduction takes place within the structure, the criteria of autopoietic self-reproduction are met [23].

Vonmont-Bachmann *et al.* [24] have investigated the reactivity of lipase, both in free solution and vesicle-entrapped, against mixed oleic acid/oleate/ethyl oleate vesicles. Enzymatic hydrolysis reaction takes place in the bilayer of the vesicle, and meets therefore the criteria of autopoiesis.

2.4.4. Formation Processes for Lipid Vesicles

Vesicles are often formed by the dispersion of lamellar bilayers where this dispersion may take place by dilution or by the input of external energy. The size distribution of the vesicles formed is typically strongly affected by the method of preparation. There are basic processes (each having many variants) discovered by means of which vesicular structure may be formed. Phospholipids which are the main amphiphiles forming the membrane of living cells have rigid bilayers. Phospholipid vesicles can be formed by sonication of aqueous dispersion of the lipid.

Vigorous shaking or vortexing may also be sufficient for the mechanical dispersion of the lipid for the homogenization of the sample yielding vesicles. [25-27]

Formation of vesicles from lipid bilayers arises due to shape and amphipathic nature of phospholipid molecules. Once formed, lipid vesicles are quite stable and, in fact, may be separated from the solution by gel filtration chromatography, or centrifugation [18]

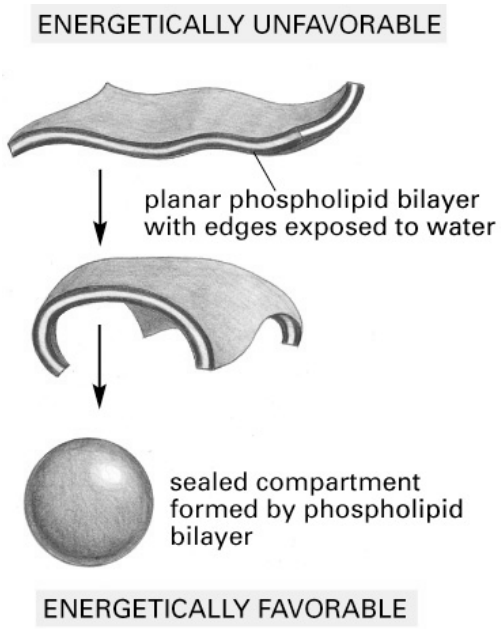


Figure 2.22. Formation of vesicle from phospholipid bilayer

A classical method is thin-film hydration where a thin film of amphiphilic material obtained by evaporation of a solution of amphiphile in chloroform or other volatile solvents with a stream of nitrogen. Subsequently this film comes into contact with water and dissolves by forming vesicles. [5, 24, 28]

Another technique for vesicle preparation is the method of high-pressure extrusion of lamellar phases. By the use of membrane filters of a given pore size, this method also allows for the formation of relatively monodisperse vesicles. [8]

Deposition of a water-insoluble surfactant onto a wetable polar solid surface followed by immersion in water yields vesicles. Wetting of the surface with displacement of adsorbed surfactant is the driving force for this process. It should also be mentioned that a chemical reaction, the acidification of a soap solution, which results in precipitation of the surfactant may produce vesicles. [16].

Finally, polymeric vesicles can be formed by polymerizable amphiphiles. This may be achieved for amphiphilic lipids that contain amino acid groups and that are polymerized through peptide bonds. [7].

2.5. Dynamics of Formation and Stability of Vesicles

Amphiphilic systems display a various phase behavior and large diversity in aggregate structures. So far it has been concerned which surfactant systems form vesicles or, which vesicles are formed spontaneously. In general, the dynamics of the formation of amphiphilic structures have not been studied intensively. Accordingly, only little is known about the structural pathways and physico-chemical parameters that control vesicle formation [4]. On the other hand, kinetic pathways and intermediate structures involved in dynamics of vesicle formation are important in colloidal science and receiving more attention to understand how this process takes place. Once, a detailed mechanism of the formation process is understood (especially in applications such as models for biological membranes, micro reactors for the preparation of inorganic nanoparticles, and vehicles for controlled release applications) then one will able to control the vesicle structures formed [29].

The structural changes may be followed by methods such as electric conductivity and turbidity, or they can be monitored with electron microscopy and scattering techniques. However, those methods can be applicable for systems that react slowly, e.g. amphiphilic block copolymers. In case of fast kinetics, a different technique such as stopped-flow technique is the method of choice [7]. The results of these techniques are well described by Smoluchowski theory for colloid coagulation. This theory includes the following steps: (1) rapid formation of disk-like or rod-like micellar intermediates, growth of these micellar aggregates, and their closure to form initial nonequilibrium vesicles, (2) subsequent vesicle growth is proceeded by slower vesicle fusion. Such disk-like precursors for the vesicles has been observed in cryo-TEM studies on phospholipid systems [29]

The various pieces of experimental evidences for the structural changes during the micelle-vesicle transition can be summarized schematically as in Figure 2.23 with rode-like and/or disc-like aggregates as intermediate structures [7].

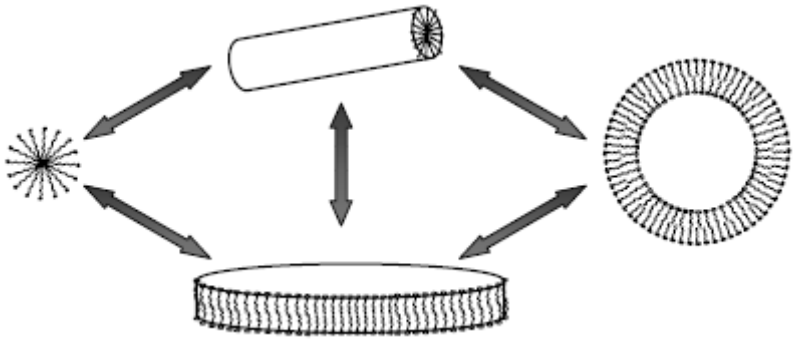


Figure 2.23. A schematic representation of pathways that may be involved in the transition form micelles to unilamellar vesicles

During the early stages of the growth process, formation of floppy bilayers takes place as a result of a modification of the effective head group area of the corresponding surfactants.

Floppy bilayers have high edge energies. These edge energies can be minimized either growth of the floppy bilayers to reduce the edge length relative to the membrane area or by bending of the bilayers to form vesicles. The critical condition for the bilayer to form vesicle is explained by Lipowsky for shape transformation of bilayer membranes [4]. The fine balance between the edge energy and bending energy determines the shape of the surfactant assembly. It has been suggested that in order to diminish the total edge energy of the aggregates, the floppy bilayers coalesce with each other until the aggregates reach a critical size at which the effect of the unstable edge overcomes the effect of the bending elastic energy. Therefore, initial nonequilibrium vesicles are formed despite the unfavorable bending energy. The transition is controlled kinetically rather than thermodynamically [7]. The thermal undulations of phospholipid bilayers are strongly dependent on the mechanical properties of the bilayer such as bending elasticity. Cholesterol, an important constituent of the living cell, incorporates in between the hydrophobic tails of the phospholipids, changes the mechanical properties of the bilayers in a manner that decrease membrane permeability by making membrane more rigid and hence improves the stability of the vesicles [1, 30].

The mechanism for growth of initial nonequilibrium vesicles is based on either fusion model, in which two vesicles coalesce to create a larger one simultaneously, or on Ostwald ripening, in which larger vesicles grow at the expense of smaller vesicles having higher curvature energies. The fusion of any two vesicles necessarily results in their loss of identity as the new vesicle is created.

Shioi and Hatton [4] have studied formation and growth of vesicles from SOS and CTAB surfactants that is followed by DLS, cryo-TEM and small-angle neutron scattering (SANS) techniques. DLS studies indicate that aggregates are larger than the original micelles in the surfactant solutions. Vesicle size distribution is determined by cryo-TEM and to verify the accuracy of the cryo-TEM size distribution SANS is performed [4, 24]. It is shown that the time required to have equilibrium vesicle size is a few months. Figure 2.24 summaries the formation and growth of vesicles in SOS/CTAB system according to the theoretical assumptions stated here.

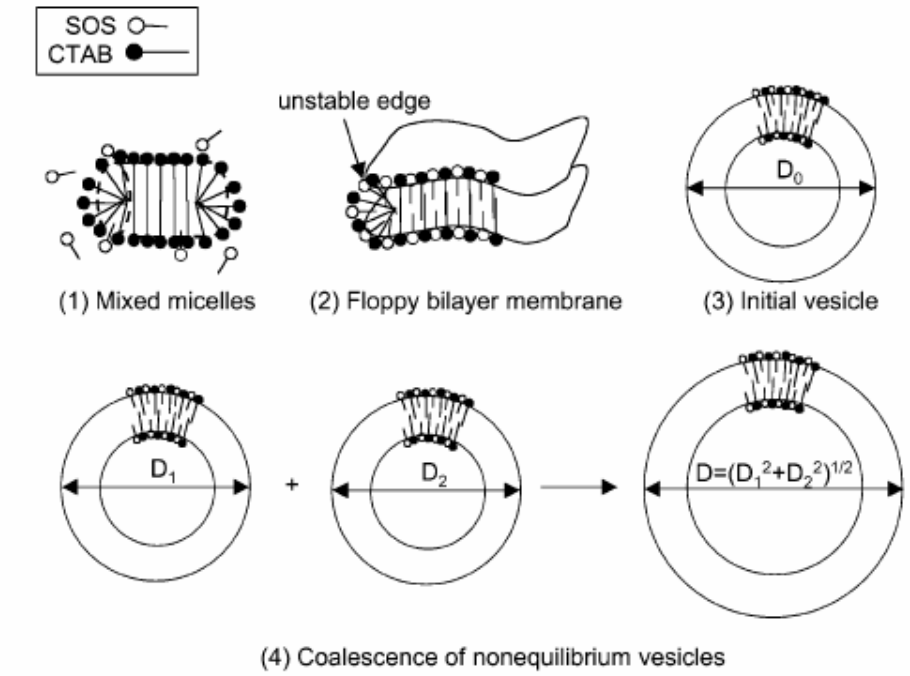


Figure 2.24. Schematic of the intermediate states that may be involved during the formation and growth of vesicles in SOS/CTAB system

2.6. Breakdown of Vesicles

Electrostatic interactions between the charged head groups play an important role in mixtures of oppositely charged surfactants and lead to the formation of variety of microstructures including vesicle phase. Unlike unilamellar vesicles formed from biological lipids, vesicles composed of oppositely charged surfactants with asymmetric chain lengths are thermodynamically stable [3, 10]. Potential application of vesicles in such roles as drug delivery of hydrophilic drugs (encapsulated in the aqueous compartment) and hydrophobic drugs (embedded within or associated with the hydrophobic portion of the bilayer) has been a growing body of literature in biological and colloidal science [1, 31-33]. The transition from vesicle to micelle is also of interest for protein reconstitution procedures, wherein a protein loaded-vesicle is solubilized to release a protein fraction [10]. For this reason, deeper understanding of the physical interactions during the transition of vesicles to micelles is needed.

It has been observed that addition of monovalent salt alters the electrostatic contribution to the free energy of aggregation and thus changes the equilibrium phase behavior. Salt addition effects in catanionic surfactant systems at some compositions are quite different from those in biological lipid systems with added salt. Brasher *et al.* [10] analyzed the breakdown of the catanionic mixture of CTAB and SOS with added sodium bromide (NaBr). They observed that a large portion of the SOS-rich vesicle lobe is destabilized to the two phase vesicle /lamellar coexistence region upon the addition of salt thus bluish turbid vesicle solution jumps to clear single phase. It seems that after addition of salt micelles become the favorite structures. QLS measurements indicate that apparent radius of CTAB/SOS vesicles (mixed in a 3:7 ratio) dramatically decreases with further addition of salt [10].

Phase diagrams provide a general method for preparing spontaneously formed vesicles of controlled size, surface charge, and permeability from commercially available surfactants. A number of papers have reported the phase diagrams of the ternary system CTAB/SOS/H_2O [2, 3, 16]. Bucak *et al.* [34] considered the rate of breakdown of catanionic vesicle system, CTAB/SOS by addition of single-chain surfactant to take the system from vesicle-stable region to micelle-stable region. As it can be seen from Figure

2.25, vesicle breakdown is achieved by mixing vesicle solution with additional SOS at high concentration to bring the system micelle-stable region.

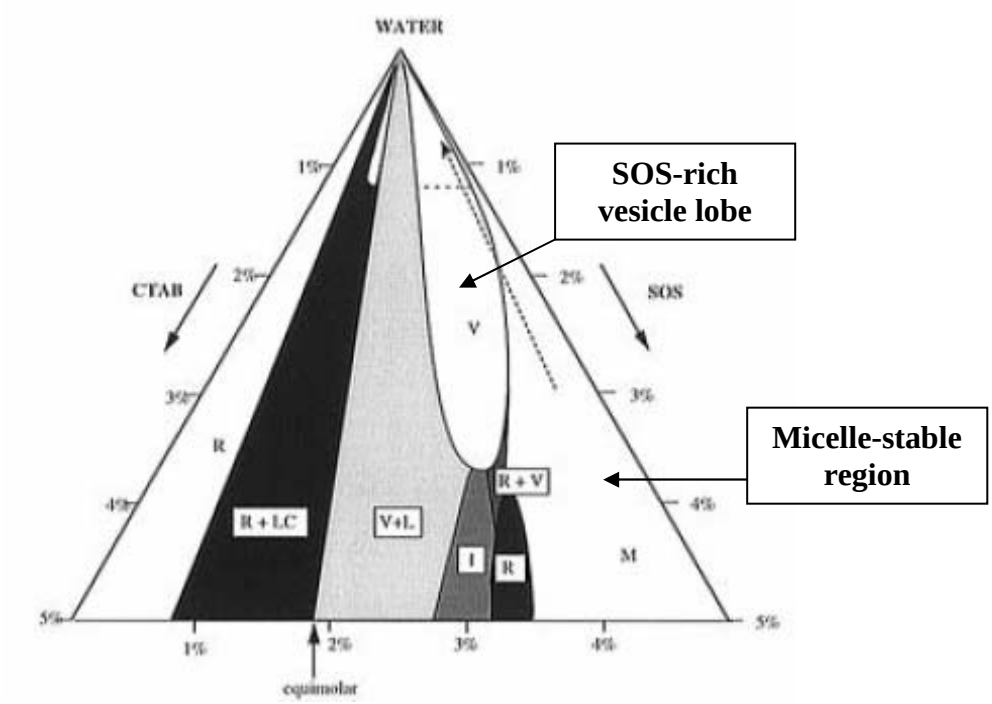


Figure 2.25. Ternary phase diagram for CTAB/SOS/H_2O at 25 ^{0}C [3]

In case of vesicles composed of (phospho)lipids, bilayer solubilization does not occur when molar ratio of salt and/or surfactant molecule in the vesicle bilayer is less than the concentration at which bilayer is saturated. The salt concentration at which the turbidity is highest taken as an estimate of salt concentration that saturates the bilayer. The condition is also acceptable for solubilization of biological lipid vesicles with surfactants. The addition of micelle-forming detergents to phospholipid vesicles can be described by a three-stage model: (1) detergent molecules partition from the aqueous phase into the bilayer leading often to a swelling and /or fusion of the vesicles. This causes an increase in vesicle size, (2) formation of mixed phospholipid/surfactant vesicles at which the vesicles are saturated with surfactant molecules depending on the phospholipid concentration, (3) at minimal total surfactant concentration vesicle solubilization takes place and no vesicle exists [8].

Solubilization of phospholipid vesicles is also possible with bile salts. Bile salts are derivatives of cholesterol that are synthesized in the liver and released by the gall bladder into the small intestines.

Malloy and Binford [25] concentrated on the titration of DMPC vesicles with a bile salt, sodium cholate. They observed rapid disruption of vesicles at a point that vesicle bilayer is almost saturated with the salt. Those bluish turbid vesicle solutions are also visibly cleared at this point.

2.7. Techniques in Vesicle Characterization

Amphiphilic molecules undergo self-assembly and form various types of self-assembled microstructures with different shape and size, and morphology. In general, multiple complementary methods are required to characterize the features of these aggregate structures. Electroscopic methods are well suited for visualization of aggregates of amphiphilic structures in aqueous environment [13].

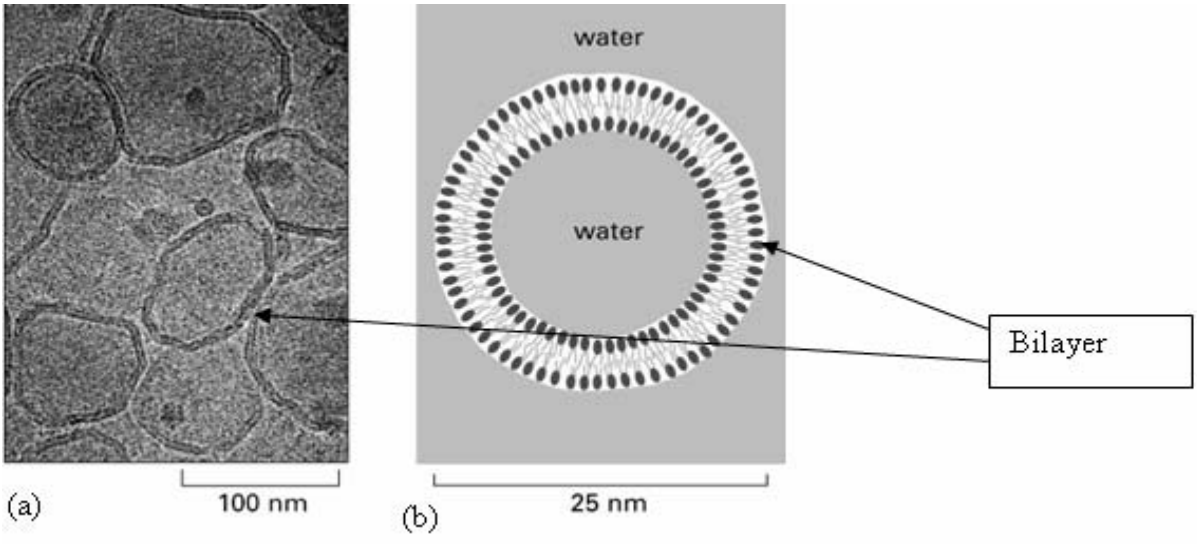


Figure 2.26. (a) Electron micrograph of thin section of phospholipid vesicles, (b) diagram of vesicle in cross section

2.7.1. Cryo-TEM

Cryo-TEM is a method allowing visualization of many fragile structures that form by self assembly of amphiphilic molecules in aqueous environment. The amphiphiles may be surfactants, lipids, or polymers. The distinctive feature of the method is that the objects are examined without dehydration. This is achieved by capturing the structures in a very thin aqueous film that is substantially turned into glass at liquid nitrogen temperatures and examined using a microscope. Objects in the size range from 5 to 500 nm are well suited for the method. This includes various emulsion particles, such as vesicles [35].

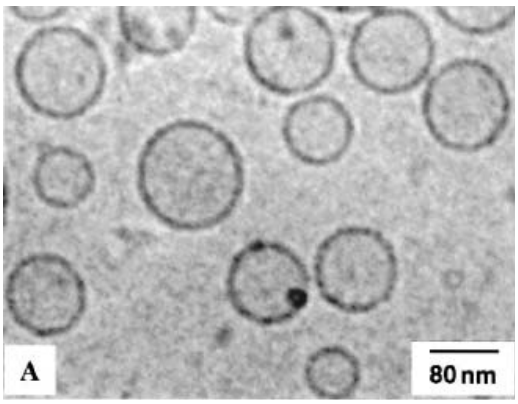


Figure 2.27. Cryo-TEM image of CTAB/SOS/H_2O

Vesicle size distribution of CTAB/SOS/H_2O is determined by cryo-TEM. For cryo-TEM a layer of vesicle liquid is spread on a carbon grid in a temperature-controlled chamber saturated with the vesicle solution of interest. The grid is cooled with by liquid nitrogen thus, sample is frozen. Then micrographs were recorded [13].

Cryo-TEM pictures of CTAT/SDBS equilibrium vesicles are obtained and the hollow nature of the vesicles is clearly visible from micrographs, and the vesicles generally appear to be spherical in shape [36].

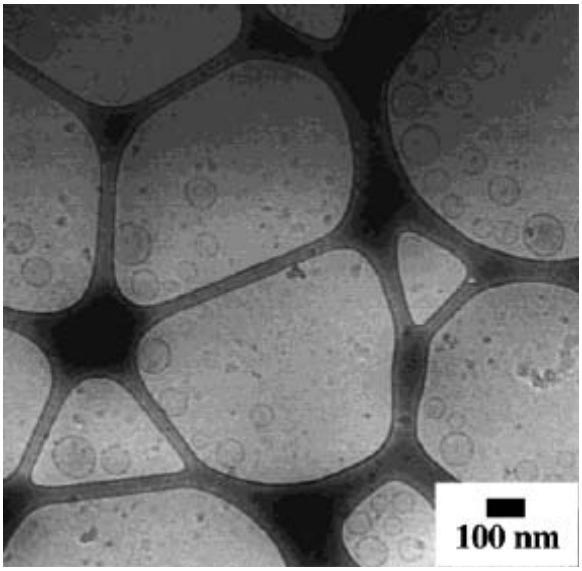


Figure 2.28. Cryo-TEM image of CTAT/SDBS vesicles

2.7.2. QLS

QLS is a non-disturbing technique which can determine the mean size and size distributions of vesicles by analysis of the fluctuations in the intensity of laser light scattering [37].

To study the transition from micelles to vesicles in SOS-rich mixtures of SOS/CTAB vesicles, the apparent aggregate size is measured using QLS. The evolution of radius with time followed by QLS is shown in Table 2.2. [3].

Table 2.2. QLS results for mixtures of CTAB and SOS, measured immediately following preparation and after aging several months [3]

		Initial preparation		**Aged preparation**	
Mixing ratio	**Surfactant (weight (wt) per cent)**	**Radius (nm)**	**polydispersity**	**Radius (nm)**	**polydispersity**
10/90	1.7	19	0.09	158	0.24
	1.4	18	0.08	134	0.26
	1.2	16	0.06	91	0.25
20/80	2.5	36	0.16	74	0.17
	2.0	19	0.13	161	0.30
	1.5	17	0.12	129	0.26
30/70	2.0	35	0.16	136	0.25

In another QLS study, the size, and size distribution of oleic acid/oleate vesicles are characterized by QLS and hydrodynamic diameter is determined as 105 nm. QLS analysis also indicates that vesicle size changes with time [24].

2.7.3. DLS

DLS is used to monitor the changes in aggregate properties with time following mixing the surfactant solutions [4]. Phospholipid vesicles of phosphatidylcholine/ hemagglutinin/ cholesterol mixtures are analyzed with DLS technique and the diameter of vesicles determined by this technique is about 24 nm [26].

2.7.4. Freeze-fracture Electron Microscopy

The most common electron microscopic technique for obtaining information on size of vesicles is freeze-fracture electron microscopy. This technique involves the size of freeze-fractured vesicles. The technique is susceptible to systematic error because only small number of images can be used to generate size distributions [38].

In case of tetradecyldimethylamine oxide (TDMAO)/ tetradecyltrimethylammonium bromide (TTABr)/ hexanol system, the freeze-fracture electron microscopy picture shows very round and well-formed vesicles [7].

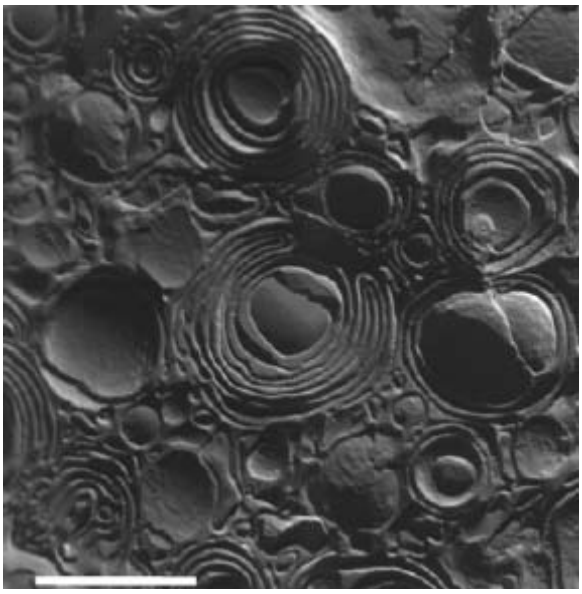


Figure 2.29. Freeze-fracture electron micrograph of MLV in TDMAO/TTABr/hexanol system

2.7.5. SANS

SANS is used to investigate the aggregate composition of vesicles. The bilayer thickness measured from SANS is found 22 Å [34].

3. REAGENTS AND INSTRUMENTS

3.1. Reagents

3.1.1. Surfactants

3.1.1.1. SDS. SDS was obtained from Sigma Chemicals Company. As an anionic surfactant it was found in white powdered form with 99 per cent purity. It was used in the formation of mixed-surfactant vesicles.

3.1.1.2. SOS. SOS was supplied from Merck as an anionic surfactant. It was used in the formation of mixed-surfactant vesicles solutions. 3 wt per cent of SOS was prepared by dissolving 3 g of SOS in 100 ml distilled water.

3.1.1.3. CTAB. Cationic surfactant CTAB with high purity (> 99 per cent) was supplied from Acros Organics to use in mixed-surfactant vesicle solutions. All *x* wt percent surfactant solutions were prepared by dissolving *x* g in 100 mL of distilled water.

3.1.2. Phospholipids

3.1.2.1. DMPC. DMPC, from Sigma Chemicals Company, was used without further purification. DMPC has a relatively hydrophobic choline head group and has 14 carbon atoms in its hydrophobic chain length. It is completely insoluble in water. The head group structure of DMPC forms a zwitterion at the working pH.

3.1.2.2. DMPG. DMPG was from Sigma Chemicals Company without further purification. The hydrophobic chain of DMPG carries 14 carbon atoms. DMPG has strong hydrophilic glycerol head group. It is negatively charged at the working and soluble in water.

3.1.3. Cytochrome-C

Cytochrome-C from bovine heart was supplied from Sigma Chemicals Company with 99 percent purity. It was used in protein encapsulation experiments.

3.1.4. Chloroform

Chloroform with purity between 99 and 99.4 per cent was supplied from Merck. It was used in preparation of phospholipid vesicles.

3.1.5. Sodium Chloride (NaCl)

NaCl was supplied from Merck. It was used to breakdown surfactant vesicles.

3.1.6. Sodium Hydroxide (NaOH)

NaOH was supplied from Ak Kimya A.S. and 0.1 M of solution was prepared to make phosphate buffer solution.

3.1.7. Potassium dihydrogen phosphate (KH_2PO_4)

KH_2PO_4 was supplied from Merck as a white powdered from. It was used in preparation of phosphate buffer solution.

3.1.8. Cholesterol

Cholesterol with high purity (> 99 per cent) was supplied from Sigma Chemicals Company. It was used in phospholipid vesicle systems.

3.1.9. Cholic Acid Sodium Salt

Cholic acid sodium salt with 99 per cent purity was supplied from Acros Organics. It was used in vesicle disruption experiments. 0.1 M of cholic acid sodium salt solutions was used in solubilization of phospholipid vesicles.

3.2. Instruments

3.2.1. pH-meter

The pH meter used was WTW Inolab pH/Cond 720. The instrument was calibrated by using buffer solutions of pH 4.00 and 7.00.

3.2.2. Water Bath

Grant thermostatic bath/ circulator W14 range 0 to 40 ^{0}C was used to keep the prepared solutions at room temperature.

3.2.3. Analytical Balance

AND GR-200 analytical balance with maximum load of 210 g and minimum load of 10 mg was used.

3.2.4. Rotary Vacuum Evaporator

BIBY R-100 rotary vacuum evaporator was used to evaporate chloroform yielding a thin lipid film.

3.2.5. Vortex Mixer

FUSION Whirlimixer was used to homogenize the suspended lipid solution.

3.2.6. Centrifuge

Rotafix 32 centrifuge was used in ultrafiltration of surfactant and phospholipid vesicles.

3.2.7. Centrifugation Filters

VIVASCIENCE Vivaspin 2 mL concentrator and MILLIPORE Centricon centrifugal filters were used in centrifugation experiments.

3.2.8. Extruder

AVESTIN Lipofast mini-extruder with two 0.25 ml Hamilton syringes (Hamilton, Reno, NV) was used with polycarbonate membranes having pore diameters of 100 nm. Phospholipid vesicles were extruded through 100 nm polycarbonate filters to have LUV of uniform size.

3.2.9. Vacuum Oven

Vacucell vacuum oven was used in order to remove residual organic solvent chloroform from the lipid film. The lipid film was left in round bottom flask under vacuum with the top open overnight.

3.2.10. UV/VIS Spectrophotometer

Turbidity and protein encapsulation analysis were measured on a TU-1880 Double Beam UV VIS Spectrophotometer. Turbidity was measured between wavelengths of 350 and 400 nm. Qualitative analysis of protein was done at 408 nm. Measurements were done with 1 cm thick quartz and polystyrene cuvettes.

Table 3.1 Parameters for UV/VIS spectrometer

Photometric Mode	Abs
Measure Mode	Single wavelength
Spectral bandwidth	2.0 nm
Coordinate Range (Abs)	0.000 to 2.000
Scanning Range (nm)	500.00 to 300.00
Lamp Status	Deuterium and Tungsten
Lamp interchange wavelength (nm)	359.90

4. EXPERIMENTAL METHODS

4.1. Preparation of Cytochrome-C in Distilled Water

Various concentrations of cytochrome-C were prepared by completely dissolving appropriate amount of protein in distilled water.

4.2. Preparation of Phosphate Buffer Solution

It was prepared by dissolving 1.36 g KH_2PO_4 in 100 mL distilled water and addition of 58.2 mL of 0.1 M NaOH (prepared by dissolving 0.4 g of NaOH in 100 mL of distilled water) followed by addition of 41.8 mL of distilled water to have 200 mL 0.05 M KH_2PO_4. The pH of the prepared buffer solution was 7.01.

4.3. Preparation of Cytochrome-C in Phosphate Buffer

Cytochrome-C was dissolved in 0.05 M phosphate buffer solution at desired concentrations.

4.4. Preparation of Sodium Cholate Solution

0.1 M sodium cholate solution was prepared by dissolving precisely weighed amount of cholic acid sodium salt in required volume phosphate buffer.

4.5. The SOS/CTAB System

Samples were prepared by first making stock solutions of each surfactant in distilled water.

4.5.1. Stock A

3 wt per cent CTAB solutions were prepared after complete dissolution of 7.5 g solid in sufficient distilled water to give 250 ml of solution. The solution was incubated at 25 ^{0}C to prevent crystallization of the surfactant.

4.5.2. Stock B

3 wt per cent SOS solution was prepared after complete dissolution of 3 g solid in sufficient distilled water to give 100 ml of solution.

The vesicle stock solution I was prepared by mixing two 3 wt per cent aqueous solutions of SOS and CTAB in a 72/28 ratio, respectively. This solution (Stock I) was then diluted by factors of 0.8, 0.6, 0.4, 0.2 to make solutions of stock II, III, IV, and V, respectively. After brief vortexing, the dispersions were not subjected to any type of mechanical agitation and they seemed bluish turbid. All the resulting solutions were then incubated at 25 ^{0}C.

4.5.3. SOS/CTAB Vesicles Containing Protein

The protein under study was the cytochrome-C which is a water soluble protein that has an isoelectric point, pI = 10.65 at 0 ^{0}C. Cytochrome-C bears a net positive charge at pH below the pI. Since SOS/CTAB system pH was measured around 7, cytochrome-C was first dissolved in negatively charged 3 wt per cent SOS solution and mixed at the desired ratio with 3 wt per cent CTAB solution to have a better encapsulation yield during vesicle formation, followed by diluting the resulting dispersions to the desired concentration.

13.9 mg cytochrome-C was dissolved in 10 mL of 3 wt per cent SOS and then 7.2 mL of this solution was separated and mix with 3.6 mL of 3 wt per cent CTAB solution to obtain stock I with a protein concentration of 0.1 mg/mL in overall solution.

4.5.4. Breakdown of SOS/CTAB Vesicles

SOS/CTAB vesicles with or without cytochrome-C were disrupted with additional SOS stock (Stock B) and NaCl solutions. Vesicle samples were titrated with SOS or NaCl until clear solutions were observed spectrophotometrically.

4.6. The SDS/CTAB System

A similar procedure has been followed for SDS/CTAB systems.

4.7. DMPC/DMPG systems

4.7.1. Preparation Method for Phospholipid Vesicles

4.7.1.1. Preparation of Lipid for Hydration. The phospholipid stock solutions were prepared by dissolving mixtures (in the molar ratio 9:1) of crystalline phospholipids (DMPC/DMPG) in chloroform to assure a homogenous mixture of lipids. The intent is to obtain a clear lipid solution for complete mixing of lipids. Once the lipids were thoroughly mixed in the chloroform, the solvent was removed by rotary evaporation yielding a thin lipid film on the sides of a round bottom flask. The lipid film was thoroughly dried to remove residual chloroform by placing the flask with the top open on a vacuum pump at room temperature overnight. The lipid film was then removed from the vacuum pump. The next step was hydration of lipid film.

4.7.1.2. Hydration of Lipid Film. Hydration of lipid film was performed simply by adding 0.05 M pH 7 phosphate buffer solution to required volume to the container of dry lipid. After addition of the hydrating medium, the lipid suspension was then maintained at 55 ^{0}C well above the phase transition temperature, T_C, of the DMPC/DMPG mixture (T_C = 20 ^{0}C) [27]. Lipid suspension was allowed to stand at 55 ^{0}C for approximately 12 hours. The product of hydration was a large, multilamellar vesicle (LMV) analogous in structure to an onion, with each lipid bilayer separated by a water layer. The solution was homogenized by vortexing the suspension for 10-20 minutes.

4.7.1.3. Extrusion. When a stable, hydrated LMV suspension was produced, the particles were downsized through a polycarbonate filter with a defined pore size by mini-extruder. Prior to extrusion through the final pore size, LMV suspensions were subjected to 10 cycles of freezing (liquid nitrogen) and thawing (37 ^{0}C water bath). This method helps prevent the membranes from clogging and improves the homogeneity of the size distribution of the final suspension. The extrusion was done about 10 ^{0}C above the T_C of the lipids. Large unilamellar vesicles by extrusion techniques (LUVETs) with 100 nm pores were generated by pressing the lipid dispersion through the 100 nm polycarbonate filter mounted in the mini-extruder fitted with two 0.5 ml Hamilton syringes (Hamilton, Reno, NV). The samples were subjected to 11 passes through the filter. An odd number of passages was performed to avoid contamination of the sample by large vesicles which might not have passed through the filter. The vesicle solutions formed were slightly turbid. Once phospholipid vesicles were produced, they were kept at 26 ^{0}C above the T_C.

4.7.2. DMPC/DMPG Vesicles Containing Protein

DMC/DMPG vesicles containing cytochrome-C was prepared by dissolving appropriate amount of cytochrome-C in the required volume of phosphate buffer prior to hydration of the dry lipid film during the preparation of the phospholipid vesicles.

4.7.3. DMPC/DMPG/Cholesterol Containing Protein

Phospholipid vesicles were prepared with the following lipid composition: DMPC/DMPG/cholesterol = 9 / 1 / 7.5 (molar ratios). Appropriate amounts of DMPC, DMPG, and cholesterol were dissolved in chloroform and thin film was obtained. The dried lipid film was then hydrated with the required volume of 0.05 M phosphate buffer containing the desired concentration of cytochrome-C. The rest of the process was the same as in the case of preparation method for phospholipid vesicles.

4.7.4. Breakdown of DMPC/DMPG Vesicles

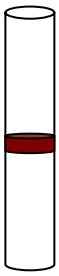
Breakdown of phospholipid vesicles with or without cholesterol and cytochrome-C was done with sodium cholate. Titration of phospholipid vesicles with sodium cholate

continued until turbidity disappeared. Turbidity analysis was followed with UV/VIS measurements.

4.8. Ultrafiltration of Surfactant and Phospholipid Vesicles

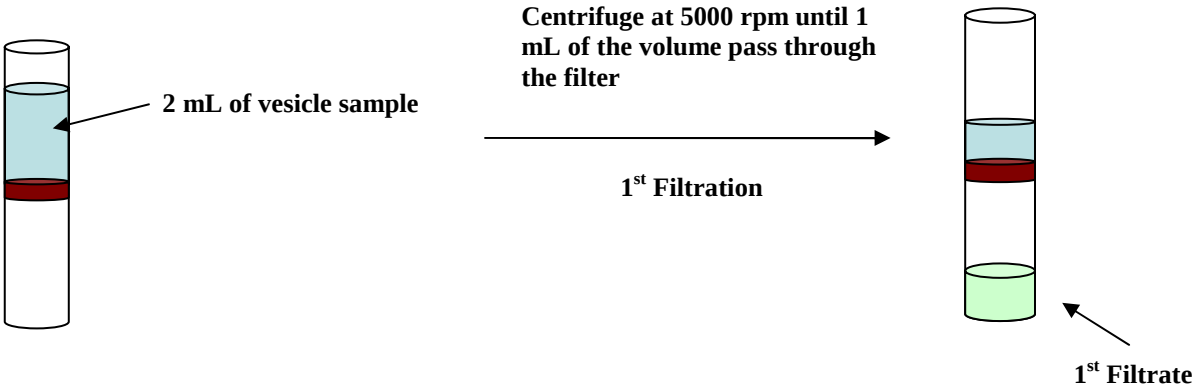
After cytochrome-C containing vesicles were prepared, the protein in the bulk (exterior of the vesicle) was removed by filtration of vesicles through Sartorius Vivaspin 2 mL ultrafiltration device containing a polyethersulfone (PES) membrane with a molecular weight cut off (MWCO) of 300 kDa (average pore radius 23 nm) and Millipore Centricon Centrifugal Filters containing a Regenerated Cellulose (RC) membrane with different MWCOs of 100 kDa and 30 kDa. It was assumed that the filters were completely permeable to non encapsulated cytochrome-C protein (has a molecular weight 12 kDa), phospholipid micelles, and cholesterol but were completely impermeable to SUV or aggregated vesicles. 2 mL of vesicle samples containing cytochrome-C were ultrafiltrated by centrifugation at different rates until half of the solution passed through the membrane of the filter. While concentrated SOS/CTAB vesicle sample containing cytochrome-C in the filtering tube was diluted with distilled water to its initial volume (2 mL) at the end of each filtration; concentrated DMPC/DMPG phospholipid vesicle sample containing cytochrome-C was diluted with phosphate buffer. Ultrafiltration of vesicle samples was repeated until no cytochrome-C observed in the filtered part. Trace of cytochrome-C in the filtrates was analyzed by spectrophotometric measurements.

4.9. Working Scheme of Ultrafiltration of DMPC/DMPG Vesicle

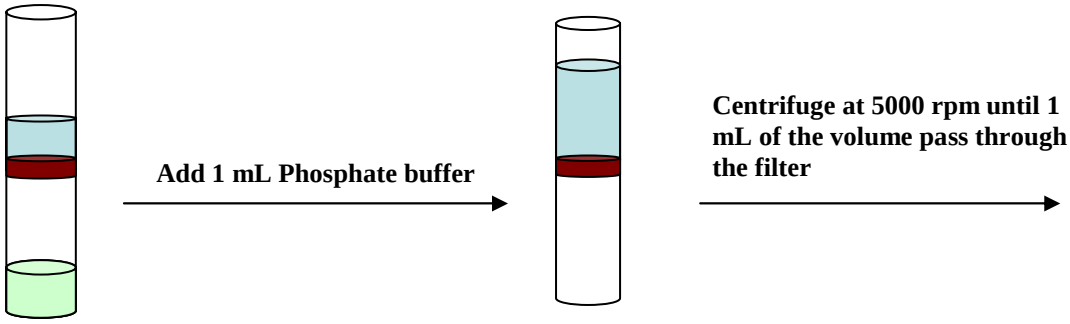


Empty Millipore filter (30 kDa)

2 mL of DMPC/DMPC phospholipid vesicle sample containing cytochrome-C was taken into the filtering tube.



1 mL of pH 7 phosphate buffer was added to restore the original volume of the vesicle sample.



This step was reapeated until no cytochrome-C was observed spectrophotometically in the filtrate.

4.10. Turbidity Measurements

Turbidity was measured on a UV/VIS double beam spectrophotometer at wavelengths of 300 and 350 nm. Sample cells were 1 cm thick quartz and polystyrene cuvettes. Cytochrome-C peak was observed at 408 nm (sometimes it was observed at 410 nm). For SOS/CTAB system distilled water was used as the reference blank solution during the turbidity measurements. In case of DMPC/DMPG phospholipid vesicle system, phosphate buffer was used as the reference blank solution.

5. RESULTS AND DISCUSSION

5.1. SOS/CTAB Systems

5.1.1. General Remarks and Visual Observations

SOS-rich vesicles were formed spontaneously at different concentrations from oppositely charged surfactants, SOS and CTAB at a mixing ratio of 72/28 respectively. The composition and concentration of the samples were well within the vesicle lobe of the ternary phase diagram of the CTAB/SOS/H_2O published by Yatchilla *et al.* [3]. The samples that were prepared at different concentrations looked similar initially, with increasing turbidity from Stock V to I as the concentration of the vesicles increased. The concentrations of SOS and CTAB in prepared stock solutions are given in Table 5.1.The stock solutions on the phase diagram are shown in Figure 5.1.

Table 5.1. Amount of SOS and CTAB in stock solutions

Stock solution	SOS wt percent	CTAB wt percent
I	2.160	0.840
II	1.728	0.672
III	1.296	0.504
IV	0.864	0.336
V	0.432	0.168

Table 5.2. pH analysis of stocks

Stock solution	pH at 25 ^{0}C
I	6.90
II	6.80
III	6.75
IV	6.74
V	6.73

As the samples aged, it was observed that the degree of turbidity changed. The change in the degree of turbidity of vesicle samples was measured on UV/VIS spectrophotometer at wavelengths of 300 and 350 nm, monthly. Samples cells used were 1 cm thick quartz cuvettes. Turbidity results of stock solutions are shown in Figure 5.2.

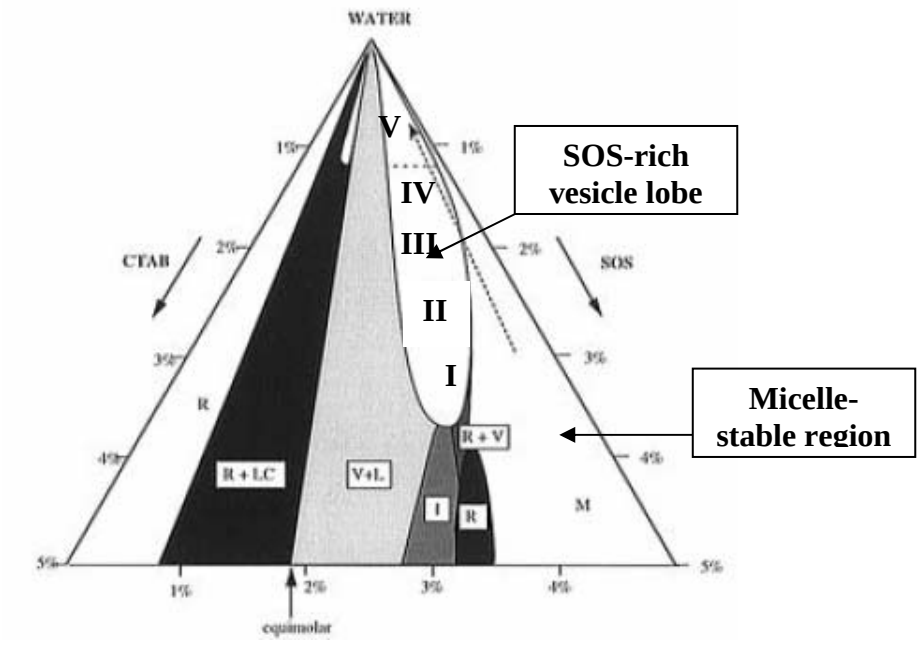


Figure 5.1. Phase diagram of SOS /CTAB/H_2O ternary systems [3]

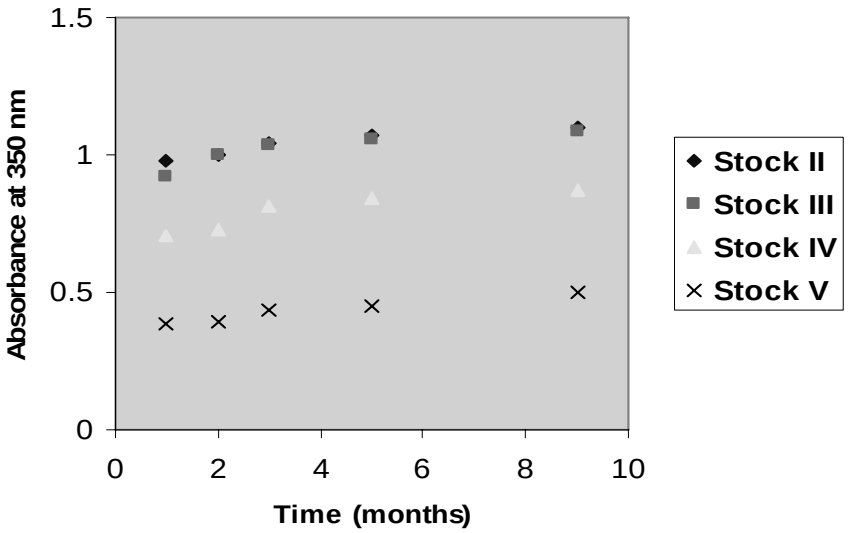


Figure 5.2. Absorbance data for Stocks II, III, IV, and V as a function of time

The increasing turbidity of SOS-rich vesicle systems as the time passed is represented in plot of absorbance versus time for different concentrations of prepared stocks. As it is seen in Figure 5.2, the increasing of absorbance indicates an increase in the degree of turbidity. Up to 3 months turbidity of samples slowly increased and it remained constant thereafter. This observed behavior is well in agreement with Bucak *et al.* [34] who have proposed that SOS/CTAB vesicles reached their final equilibrium state in 3 months.

All the samples seemed stable for at least 6 months. After 6 months, precipitation was observed in Stock III, IV, and V. This precipitation might arise from the formation of cetyltrimethylammoniumoctylsufate. Only Stock II was free of precipitate during one-year period of time.

5.2. Breakdown of SOS/CTAB Vesicles with SOS

Stock II vesicle solution with/without cytochrome-C was prepared. 2 mL of these samples were titrated with Stock B.

3.5 mg cytochrome-C was weighed and dissolved in 10 mL of Stock B. 7.2 mL of this solution was mixed with 3.6 mL of Stock A to obtain 10 mL of Stock I containing 0.25 mg/mL cytochrome-C. This solution was then diluted by a factor of 0.8 to have Stock II containing 0.2 mg/mL cytochrome-C.

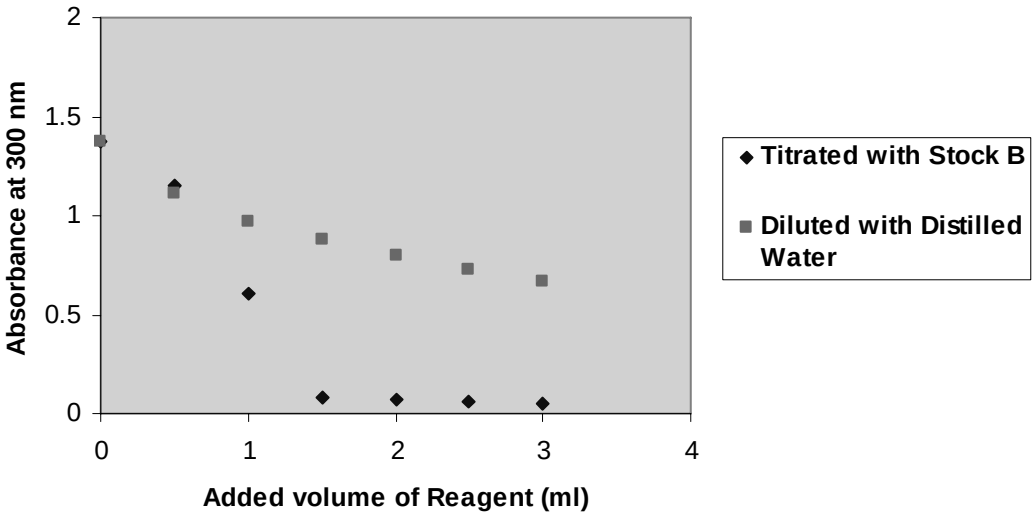


Figure 5.3. Absorbance of Stock II at 300 nm as a function of added Stock B, and distilled water

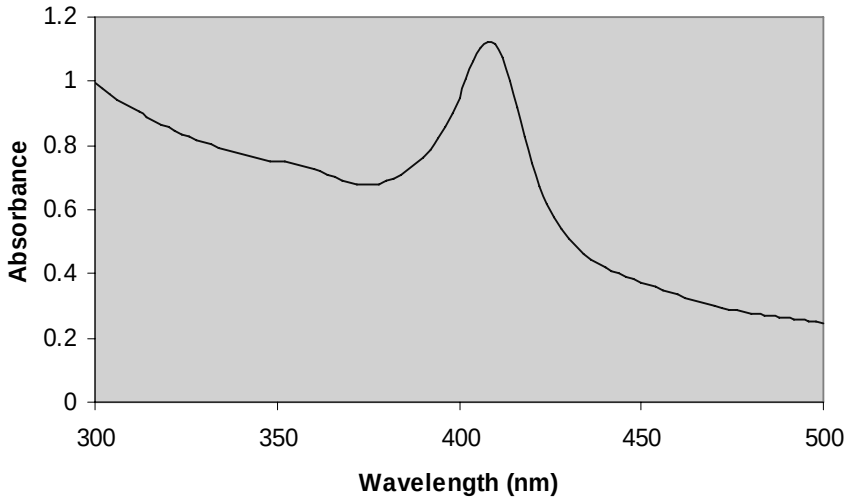


Figure 5.4. Absorbance versus wavelength plot of Stock II containing 0.2 mg/mL cytochrome-C after addition of 2 mL distilled water

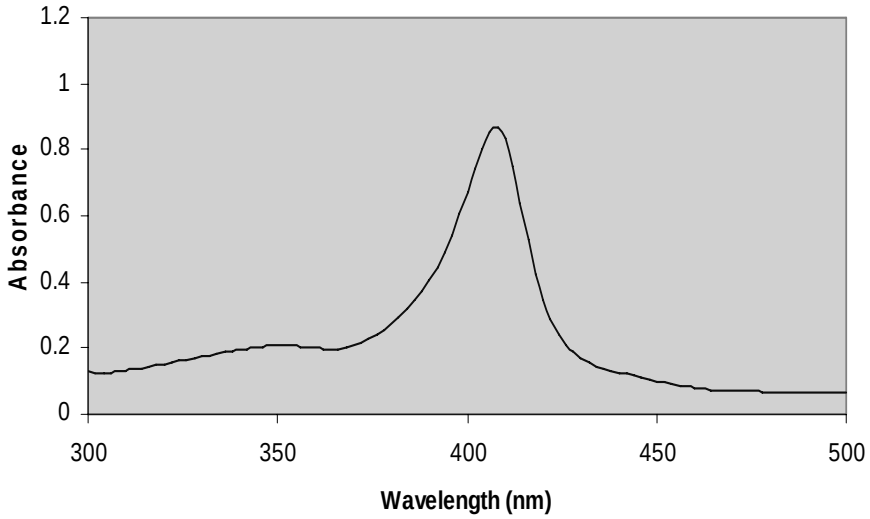


Figure 5.5. Absorbance versus wavelength plot of Stock II containing 0.2 mg/mL cytochrome-C after addition of 2 mL Stock B

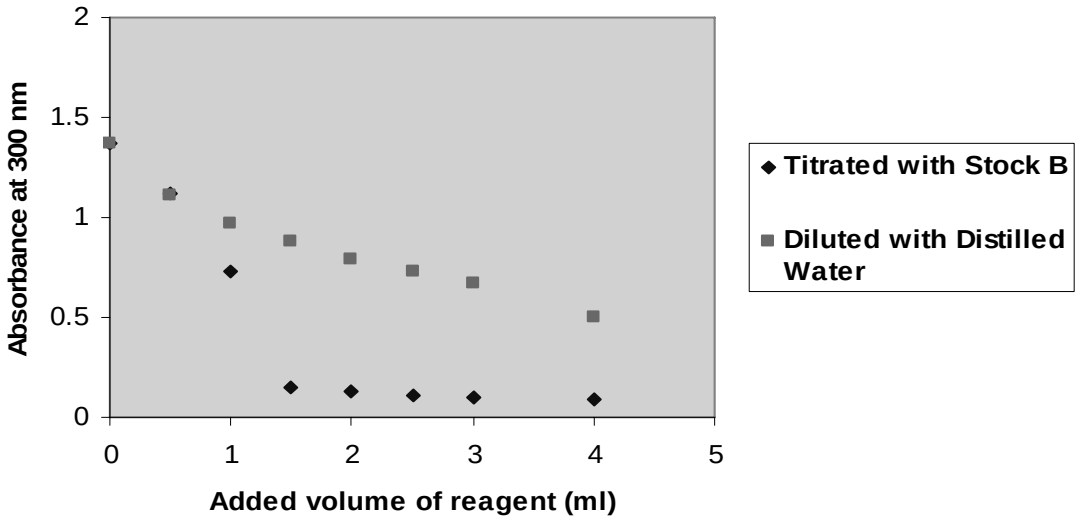


Figure 5.6. Absorbance of Stock II at 300 nm containing cytochrome-C as a function of added Stock B, and distilled water

Vesicle breakdown was achieved by mixing vesicle solution with additional SOS to take the system into the micelle-stable region (see Figure 5.1.). The turbidity of vesicle sample after each time known volume of SOS added was measured on UV/VIS spectrophotometer and the results are shown in Figures 5.3 and 5.6. Dilution effect was

also considered and the change in turbidity was checked after addition of distilled water as well as addition of same volume of SOS solution at each step. Although there is a slow decrease in turbidity when the vesicle sample is diluted with distilled water, the degree of turbidity sharply decreases at some point in Figures 5.3. and 5.6. by addition of Stock B and the final solution became completely clear. The breakdown of vesicles, therefore, can be followed by means of the turbidity change on a UV/VIS spectrophotometer. In both Figure 5.3. and 5.6, there is higher result than expected when 1 mL of reagent was added to breakdown the vesicles with/without cytochrome-C. This point probably indicates the transition of vesicles to micelles as shown in Figure 2.23.

Absorbance response of cytochrome-C in Stock V, prepared by diluting Stock I containing 1 mg/mL cytochrome-C by a factor of 0.2, was recorded for a sample titrated with Stock B and for a sample diluted with the same amount of distilled water. The results are given in Table 2.

Table 5.3. Absorbance change of cytochrome-C upon vesicle breakdown

Added volume of reagent (mL)	**Absorbance response of cytochrome-C at 408 nm**	
	Stock V containing 0.2 mg/mL cytochrome-C titrated with Stock B	**Stock V containing 0.2 mg/mL cytochrome-C diluted with distilled water**
0.0	1.611	1.611
2.6	0.804	0.804
3.5	0.756	0.762

The results given in Table 5.3 shows that protein absorbance signals in Stock V are more or less the same in two cases.

5.3. Breakdown of SOS/CTAB Vesicles with NaCl

Two mL of vesicle samples, initially prepared with/without cytochrome-C, were titrated with 1 M NaCl solution. The results were compared with the change in turbidity of vesicles in case of dilution with distilled water.

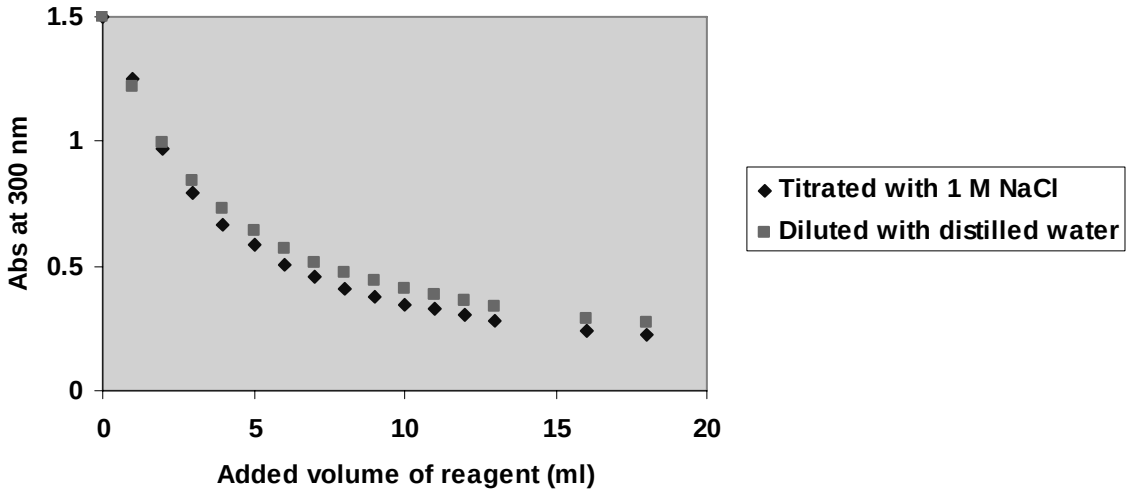


Figure 5.7. Absorbance of 2 mL Stock II containing cytochrome-C at 300 nm as a function of added NaCl, and distilled water

The turbidity of vesicle sample was measured on UV/VIS spectrophotometer after each time known volume of electrolyte solution was added. The results are shown in Figure 5.7. It seems that there is little difference in turbidity in both cases. Considerable decrease in turbidity might be observed after samples were equilibrated for several months as Brasher *et al.* [10] suggested.

5.4. DMPC/DMPG Phospholipid Vesicles

Different concentrations of phospholipids forming vesicles were prepared with/without cytochrome-C and cholesterol throughout the experiments. Phospholipids DMPC and DMPG were mixed in the molar ratios of 8.5/1.5 and 9/1 respectively. The vesicle solutions formed were slightly turbid and dispersions of phospholipids prior to extrusion were not homogeneous at all. Aggregation was observed the day after vortexing

the samples. Aggregated vesicles were discarded simply by filtering the sample by using filtering papers. Turbidity of phospholipid vesicles remained the same for at least two weeks.

The ‘‘initial’’ compositions of prepared phospholipid vesicles are recorded in Table 5.4. However, since there was precipitation in all solutions, the actual concentrations are different and impossible to know.

Table 5.4. Compositions of phospholipid vesicles

Samples	**DMPC (mM)**	**DMPG (mM)**	**DMPC/DMPG molar ratio**	**Cytochrome-C (mg/mL)**	**Cholesterol (mg)**
S1	5.0	0.88	9/1	0.4	16.1
S2	5.0	0.88	9/1	0.4	---
S3	5.0	0.88	9/1	---	---
S4	2.0	0.35	8.5/1.5	0.4	---

5.5. Breakdown of DMPC/DMPG Vesicles

DMPC/DMPG phospholipid vesicles were titrated with sodium cholate at room temperature. Malloy and Binford [25] showed that solubilization of DMPC/DMPG vesicles is possible when bilayer is saturated with bile salt. A sharp drop in absorbance was observed as incremental addition of bile salt, sodium cholate. These suspensions also visibly cleared after addition of sodium cholate.

Titration of 1 mL S1 and S2 samples were performed with 0.1 M sodium cholate solution. Another 1 mL of those samples was also diluted by incremental addition of buffer to compare the dilution effect. Data were always collected 15 second after mixing the added volume of reagent with the samples followed by rapid shaking.

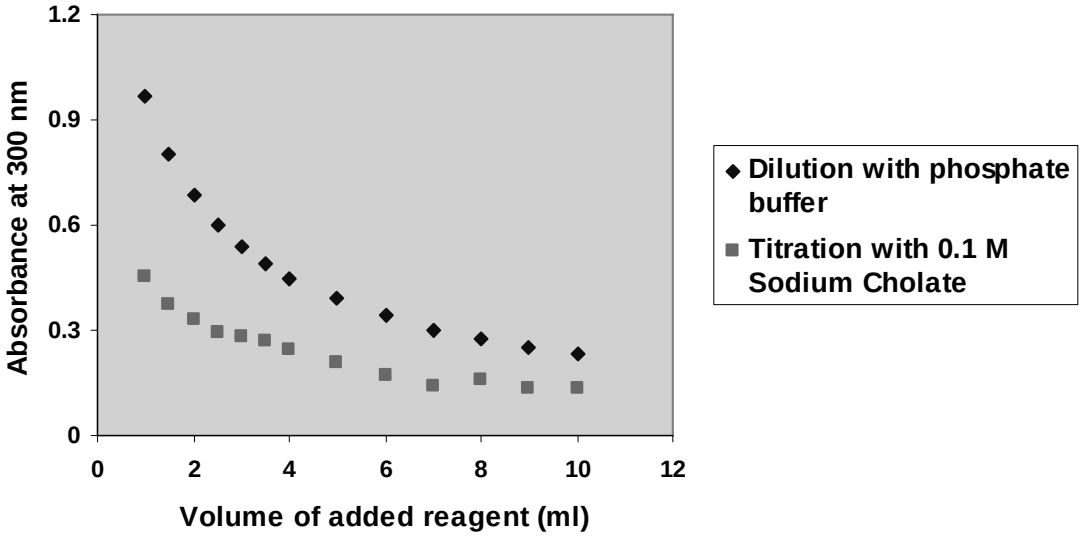


Figure5.8. Absorbance at 300 nm for 1 mL S1 as a function of added 0.1 M sodium cholate, and phosphate buffer

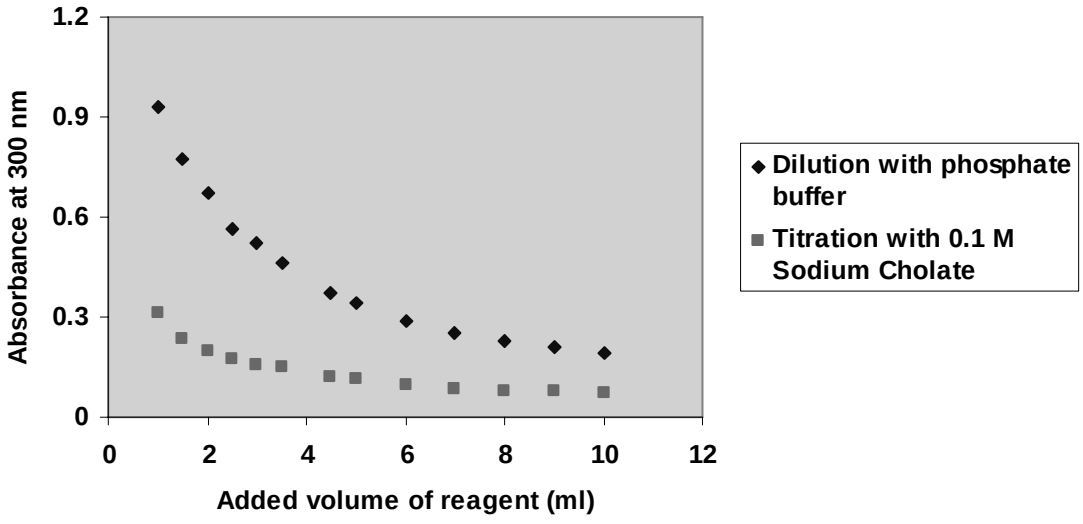


Figure5.9. Absorbance at 300 nm for 1 mL S2 as a function of added 0.1 M sodium cholate, and phosphate buffer

When S1 and S2 phospholipid vesicle samples were titrated with 0.1 M sodium cholate, the decrease in the absorbance was observed as shown in Figures 5.8. and 5.9. This is due to the saturation of vesicle bilayer with excess amount of sodium cholate, yielding solubilization of bilayer, followed by breakdown of vesicles. These results are also in agreement with those observed by Maloy and Binford [25].

The decrease in concentration for cytochrome-C in S1 was also observed with the change in absorbance at 408 nm throughout the titration and dilution trials of S1.

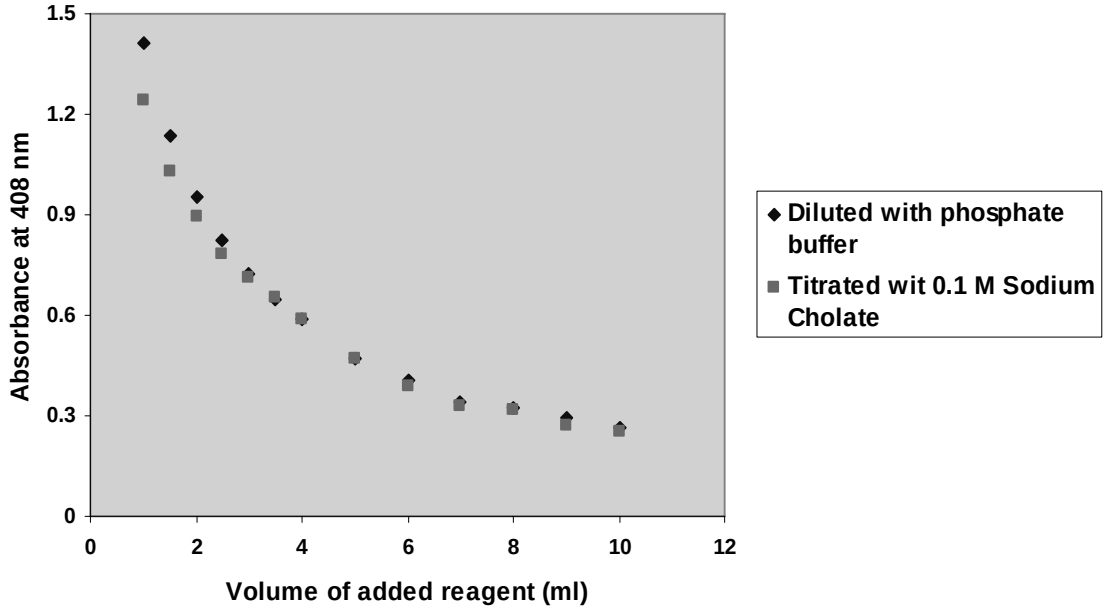


Figure 5.10. Absorbance for cytochrome-C at 408 nm in S1 as a function of added 0.1 M sodium cholate, and phosphate buffer

Protein absorbance signal was always higher in vesicle systems than it was in phosphate buffer or aqueous solutions. The absorbance data were collected for cytochrome-C throughout titration and dilution experiments of S1. As it is shown in Figure 5.10, it was observed that absorbance data collected at 408 nm during titration of S1 with 0.1 M sodium cholate well fitted with the one collected during the dilution of the same sample when protein absorbance signal fell below 0.7. Returning back to Figure 5.8. with

these results, it is concluded that at lower absorbance values (Abs < 0.6), correlated with turbidity of vesicles, cytochrome-C signal was almost the same at those turbidity levels.

5.6. Ultrafiltration of Vesicles Containing Cytochrome-C

Both SOS/CTAB and DMPC/DMPG vesicles containing cytochrome-C were filtrated with two different ultrafiltration devices. The technical specifications of those materials are given in Table 5.5.

Table 5.5. Technical specifications of ultrafiltration devices

Technical Specifications	**Sartorius Vivaspin 2 Ultrafiltration Concentrator**	**Millipore Centricon Centrifugal Filter**
Start Volume, mL	2	2
Hold-up Volume, µl	< 10	20
Membrane	PES	RC
Filtration Area, cm^2	1.20	0.92
MWCO, kDa	300	30 and 100

5.6.1. Ultrafiltration of SOS/CTAB Vesicles Containing Cytochrome-C

Stock solutions of SOS/CTAB vesicles containing cytochrome-C were prepared at desired concentrations (0.2 mg/mL, 0.4 mg/mL, and 1.0 mg/mL) by dissolving appropriate amount of protein in the required volume of Stock B then mixing with enough Stock A. Two mL of each stock was pipetted in either Vivaspin 2 Ultrafiltration Concentrator or Centricon Centrifugal Filter (100 kDa) and centrifuged at 3000, 4000, and 5000 rpm values to eliminate free cytochrome-C in the exterior of the vesicles in the bulk. Time to concentrate the vesicle sample two fold was between 1 and 2 hour. Ultrafiltration of samples was done according to the working scheme illustrated for DMPC/DMPG vesicles. SOS/CTAB vesicles were not extruded prior to ultrafiltration process. Each filtrate was analyzed in UV/VIS spectrophotometer at 408 nm for its cytochrome-C content.

The absorbance of turbidity was not higher than 0.5, meaning that vesicle penetration through the membrane was tolerable. As ultrafiltration process went on, a tendency of decrease in absorbance was recorded for cytochrome-C in the latter filtrates up to third round of filtration. However, after third round of filtration, aggregation of vesicles took place, followed by dilution of vesicle sample to its initial volume. The same problem was observed for all stocks of SOS/CTAB at this stage. Another important problem was clogging of PES membrane of Vivaspin 2 Ultrafiltration Concentrator with cytochrome-C and, therefore, ultrafiltration of SOS/CTAB vesicles did not work with this method.

5.6.2. Ultrafiltration of DMPC/DMPG Vesicles Containing Cytochrome-C

Ultrafiltration of phospholipid vesicle S4 was done with Vivaspin 2 Ultrafiltration Concentrator at 4000 rpm. Two mL of S4 extruded prior to ultrafiltration pipetted in to the filtering device (MWCO 300 kDa) and it was observed that the entire sample passed through the membrane in less than 10 minutes and filtrate was quite turbid and also fouling of membrane due to protein adsorption was again observed in the case of ultrafiltration of S4. Since these unexpected results were obtained, further experiments were carried out using Millipore Centricon Centrifugal filters with 30 kDa MWCO in the ultrafiltration experiments.

Ultrafiltration of S1 and S3 gave satisfactory results with Millipore Centricon Centrifugal 30 kDa MWCO filters. Each filtrate was labeled as SXFY where, X is the sample number and Y represents order of filtrates from the beginning to the final one. Complete removal of free cytochrome-C from S3 was achieved at the end of ten filtrations. The cytochrome-C concentration in the filtrates decreased in the latter filtrations. At the end of tenth filtration (in S3F10), no trace cytochrome-C was recorded at 408 nm (see Figure 5.11. and 5.12). The absorbance response of cytochrome-C at 408 nm in the filtrates was plotted in Figure 5.11.

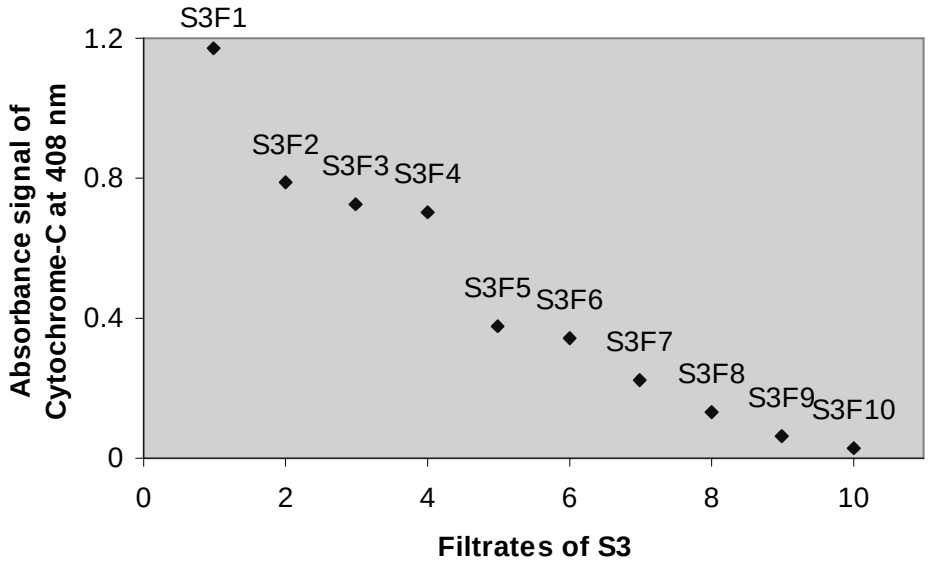


Figure 5.11. Absorbance of cytochrome-C at 408 nm for filtrates of S3

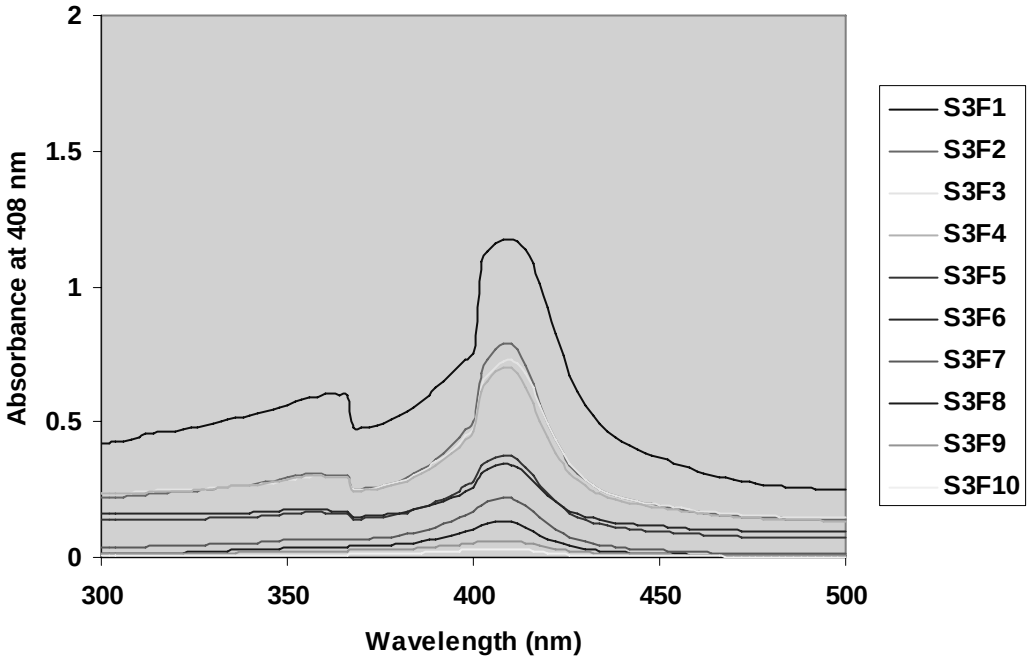


Figure 5.12. Absorbance versus wavelength plot of Filtrates of S3

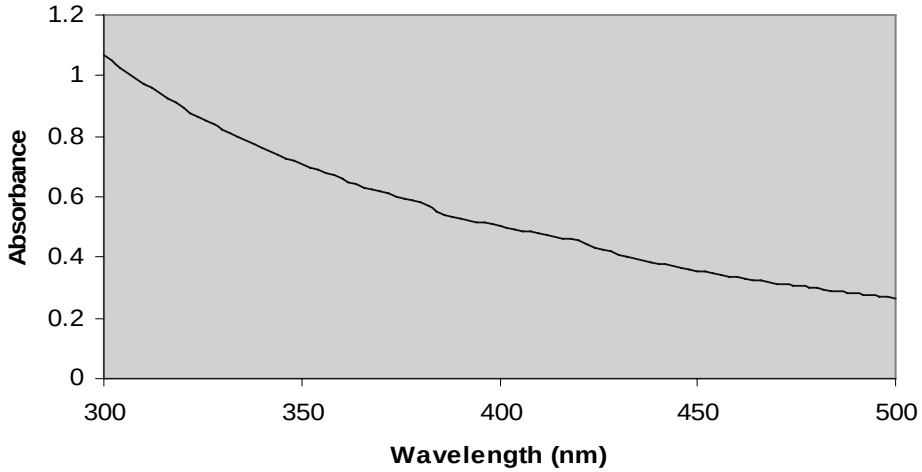


Figure 5.13. Absorbance versus wavelength plot of S3 after ultrafiltration

Absorbance measurement of S3 filtrates in Figure 5.12. indicates that concentration of cytochrome-C decreases after each filtration. This means that there is no free cytochrome-C outside of the vesicles.

Absorbance measurement of S3 when ultrafiltration was completed was given in Figure 5.13. No cytochrome-C peak was observed at 408 nm. The reason might arise from leakage of encapsulated protein from the vesicle as the exterior concentration of protein decreased.

Ultrafiltration of S1 was also under consideration for protein encapsulation capacity study. Two mL of S1 filtrated through 30 kDa Millipore Centricon Centrifugal filtering device until protein signal measured in the latter filtrate was almost zero. The results of this study are shown in Figures 5.14, 5.15, and 5.16.

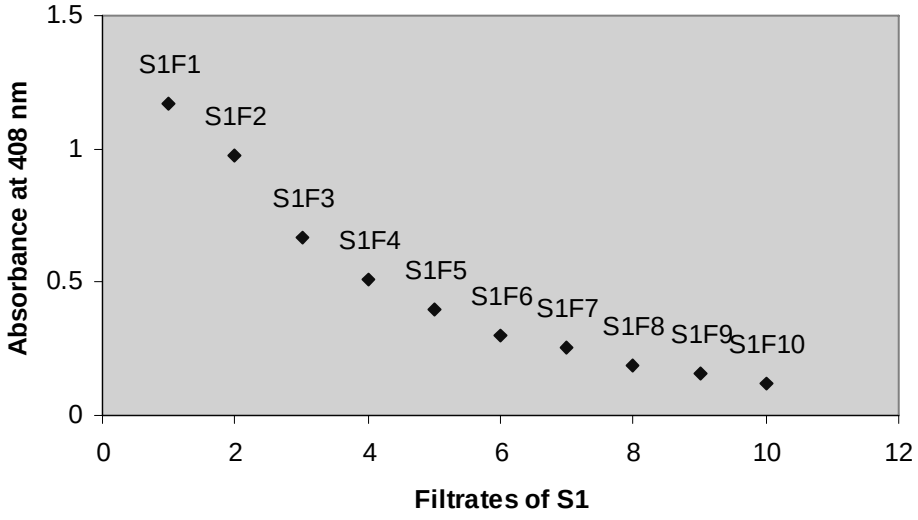


Figure 5.14. Absorbance of cytochrome-C measured at 408 nm wavelength for filtrates of S1

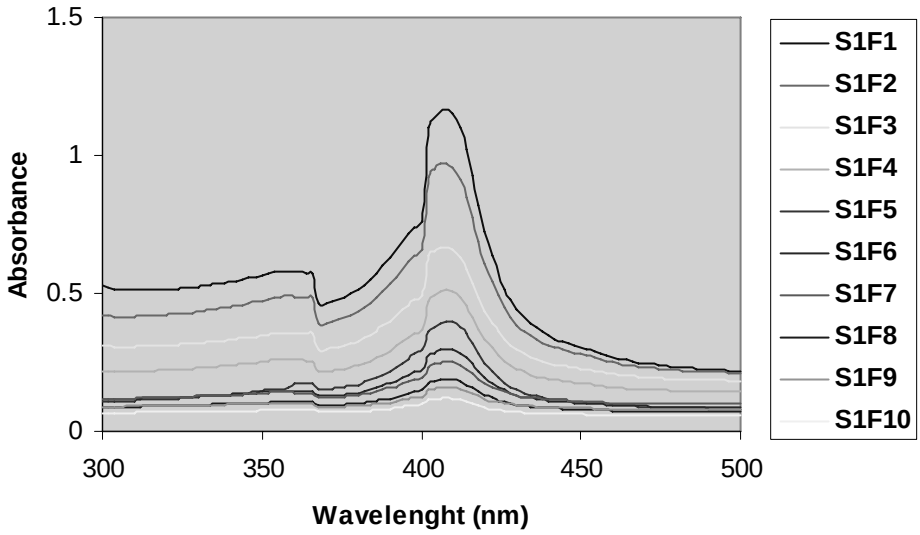


Figure 5.15. Absorbance versus wavelength plot of Filtrates of S1

After ultrafiltration of S1 repeated 10 times, the concentrated S1 seemed in the light color of protein. This observation has suggested that although free proteins outside of the vesicles were gone away through the membrane, at least one protein was encapsulated within the vesicles.

In order to recover the encapsulated protein in the filtrate the following procedure was applied: (a) the 1 mL of S1 solution, obtained after tenth filtration, was mixed with 1 mL of 0.1 M sodium cholate to bring it back to the original volume, (b) Addition of sodium cholate resulted in the breakdown of the vesicle, (c) the solution was filtered once more to recover the encapsulated protein in the filtrate, (d) finally, the filtrate was observed spectrophotometrically.

The protein signal is shown as the red signal in Figure 5.16, the remaining ‘‘black’’ signals are the same ones in Figure 5.15. As can be seen from Figure 5.16., the protein signal is quite higher to consider protein encapsulation capacity of DMPC/DMPG systems.

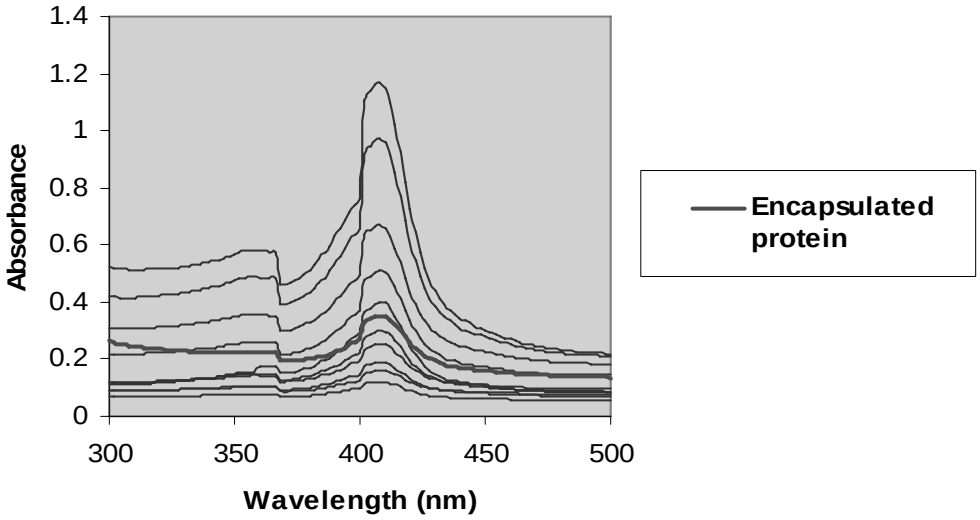


Figure 5.16. Absorbance wavelength plot of encapsulated cytochrome-C

6. CONCLUSION

In this study, investigation was focused on modeling drug encapsulation using two vesicle systems: (1) spontaneously formed SOS/CTAB surfactant vesicles, (2) DMPC/DMPG phospholipid vesicles. Distribution of cytochrome-C in these systems was observed at 408 nm on UV/VIS spectrophotometer.

SOS/CTAB vesicles at different concentrations within the vesicle lobe of the ternary phase diagram seemed to be stable for at least 6 months. It has been shown that SOS/CTAB vesicle breakdown is possible with additional SOS. Disintegration of SOS/CTAB vesicles can also be achieved with NaCl but it is observed that it takes long time (several months).

Phospholipid vesicles prepared at different concentration of DMPC and DMPG phospholipids according to the method described in the experimental part. Aggregation observed in these dispersions prior to extrusion, actual concentrations of phospholipids were not the same with ‘‘initial’’ compositions.

Breakdown of DMPC/DMPG vesicles was achieved by addition of sodium cholate. The turbid suspension became completely clear just after addition of sodium cholate. A sharp drop in absorbance was observed as incremental addition of sodium cholate.

Ultrafiltration of SOS/CTAB and DMPC/DMPG vesicles containing cytochrome-C was done with two different filters to isolate vesicles from non-trapped cytochrome-C. It was observed that the filter with PES membrane is not suitable for ultrafiltration of vesicles containing cytochrome-C because of adsorption of protein on to the membrane followed by clogging of the membrane. This problem was not observed in the case of other filter having RC type membrane.

It was also observed that SOS/CTAB vesicles are not stable enough as DMPC/DMPG vesicles because during the ultrafiltration experiments performed between 2000-5000 rpm values vesicle aggregation was observed in SOS/CTAB vesicles.

DMPC/DMPG vesicles with/without cholesterol seemed to be stable during the ultrafiltration.

At the end of ultrafiltration of DMPC/DMPG vesicles containing cytochrome-C with/without cholesterol, perturbation of vesicles was done with sodium cholate. No encapsulated protein was observed in the vesicles with any cholesterol. However, considerable cytochrome-C protein signal was observed with in the DMPC/DMPG system prepared with cholesterol. Cholesterol is often incorporated conventional lipid vesicle formulations to help decrease membrane permeability by making membrane more rigid and hence improves stability. Therefore, it is concluded that cholesterol in the bilayer prevents the leakage of protein in the vesicle.

These remarkable results showed that our method is suitable for modelling of drug encapsulation. Other preparation methods can be used to obtain homogenous DMPC/DMPG vesicles for quantitative analysis in protein encapsulation experiments.

7. SUGGESTIONS FOR FUTURE WORK

1. Formation of vesicles from natural surfactants could not be followed quantitatively due to undesired vesicle aggregation in the case of DMPC/DMPG vesicles. The preparation method should be improved in order to obtain stable samples with precisely known concentrations, so that quantitative results can be obtained.

2. Having achieved protein encapsulation in DMPC/DMPG vesicles, now a series of suitable drugs should be entrapped within these systems. Since the ultimate aim is to design an “ideal” drug-delivery system, encapsulation of a chemokine-receptor should also be tried.

3. The nature of the biocompatible natural surfactants should be changed in order to have a wide choice of vesicles in the drug encapsulation modelling studies. Entrapment of both proteins and drugs should be followed in these new systems.

8. REFERENCES

1. Patel, G. B. and G. D. Sprott, "Archaeobacterial Ether Lipid Liposomes (Archaeosomes) as Novel Vaccine and Drug Delivery Systems", *Critical Reviews in Biotechnology,* Vol. 19, Iss. 4, pp. 317-357, 1999.

2. Kaler, E. W., K. L. Herrington and A. K. Murthy, "Phase Behavior and Structures of Mixtures of Anionic and Cationic Surfactants", *J. Phys. Chem.*, Vol. 96, pp. 6698-6707, 1992.

3. Yatcilla, M. T., K. L. Herrington, L. L. Brasher and E. W. Kaler, "Phase Behavior of Aqueous Mixtures of Cetyltimethylammonium Bromide (CTAB) and Sodium Octyl Sulfate (SOS)", *J. Phys. Chem.,* Vol. 100, pp. 5874-5879, 1996.

4. Shioi, A. and T. A. Hatton, "Model for Formation and Growth of Vesicles in Mixed Anionic/Cationic (SOS/CTAB) Surfactant Systems", *Langmuir*, Vol.18, pp. 7341-7348, 2002.

5. Goldmann, W. H., R. Senger, S. Kaufmann and G. Isenberg, "Determination of the Affinity of Talin and Vinculin to Charged Lipid Vesicles: A Light Scatter Study" '', *FEBS Letters*, Vol. 368, pp.516-518, 1995.

6. Zhai, L., X. Lu, W. Chen, C. Hu and L. Zheng, "Interaction between Spontaneously Formed SDBS/CTAB Vesicles and Polymer Studied by Fluorescence Method", *Colloids and Surfaces A: Physicochem. Eng. Aspects*, Vol. 236, pp.1-5, 2004.

7. Gradzielski, M., "Vesicles and Vesicle Gels –Structure and Dynamics of Formation", *J. Phys. Condense Matter*, Vol. 15, pp. 655-697, 2003.

8. Treyer, M., P. Walde and T. Oberholzer, "Permeability Enhancement of Lipid Vesicles to Nucleotides by use of Sodium Cholate: Basic Studies and Application to

Enzyme-catalyzed Reaction Occurring inside the Vesicles", *Langmuir*, Vol. 18, pp.1043-1050, 2002.

9. Kokkona, M., P. Kallinteri, D. Fatouros and S. G. Antimisiaris, "Stability of SUV Liposomes in the Presence of Cholate Salts and Pancreatic Lipases: Effect of Lipid Composition", *European J. Pharmaceutical Sci*., Vol. 9, pp.245-252, 2000.

10. Brasher, L. L., K. L. Herrington and E. W. Kaler "Electrostatic Effects on the Phase Behavior of Aqueous Cetyltrimethylammonium Bromide and Sodium Octyl Sulfate Mixtures with Added Sodium Bromide", *Langmuir*, Vol. 11, pp.4267-4277, 1995.

11. Sanchez-Ferrer, A. and F. Garcia-Carmona, "Reverse Vesicles as a New System for Studying Enzymes in Organic Solvents", *Biochem. J*., Vol. 285, pp. 373-376, 1992.

12. Kunitake T. and Y. Okahata, "A totally Synthetic Bilayer Membrane", *J. Am. Chem. Soc*., Vol. 99, pp. 3860–3861, 1977.

13. Karukstis, K. K., S. A. McCormack, T. M. McQueen and K. F. Goto, "Fluorescence Delineation of the Surfactant Microstructures in the CTAB-SOS-H_2O Catanionic System", *Langmuir*, Vol. 20, pp.64-72, 2004.

14. Marques, E. F., "Size and stability of catanionic vesicles: Effects of formation path, sonication, and aging", *Langmuir*, Vol. 16, Iss.11, pp. 4798-4807, 2000.

15. Luk, Y.Y. and N. L. Abbott, "Applications of functional surfactants", *Current Opinion in Colloid and Interface Sci*., Vol. 7, pp. 267-275, 2002.

16. Laughlin, R. G., "Equilibrium Vesicles: Fact or Fiction", *Colloids and Surfaces A: Physicochem. Eng. Aspects*, Vol. 128, pp. 27-38, 1997.
17. Voet, D., J. G. Voet and C. W. Pratt, "Fundamentals of *Biochemistry", Second Edition*, John Wiley and Sons, Inc., NJ, 2006.

18. Nelson, D. L. and M. M. Cox, *"Lehninger Principles of Biochemistry", Third Edition*, Worth Publishers, NY, 2000.

19. Bangham, A. D., M. M. Standish and J. C. Watkins, "Diffusion of Univalent Ions Across Lamellae of Swollen Phospholipids", *J. Molec. Biol*., Vol. 13, Iss.1, pp. 238-252, 1965.

20. Helenius A. and K. Simons, "Solubilization o f Membranes By Detergents", *Biochim. Biophys. Acta*, Vol. 415, Iss.1, pp. 29-79, 1975.

21. Jackson, M. L., C. F. Schmidt, D. Lichtenberg, B. J. Litman and A.D. Albert, "Solubilization of Phosphatidylcholine Bilayers by Octyl Glucoside", *Biochemistry*, Vol. 21, Iss.19, pp. 4576-4582, 1982.

22. Binford, J. S. and L. Wadso, "Calorimetric Determinatıon of The Partition-Coefficient for Chlorpromazine Hydrochloride in Aqueous Suspensions of Dimyristoylphosphatidylcholine Vesicles", *J. Biochem. Biophys. Methods*, Vol. 9, Iss. 2, pp. 121-131, 1984.

23. Fleischaker, G. R. (ed.), "*Self Production of Supramolecular Structures*", pp. 209-216, Kluwer Academic Publishers, 1994.

24. Vonmont-Bachmann, P. A., P. Walde and P. L. Luisi, "Lipase-catalyzed Reactions in Vesicles as an Approach to Vesicles Self-Reproduction", *J. Liposome Research,* Vol. 4, Iss. 3, pp. 1135-1158, 1994.

25. Malloy, R. C. and J. S. Binford, Jr., "Enthalpy Titration and Solibilization of Dimyrostylphosphatidylcholine Vesicles with Bile salts", *J. Phys. Chem.,* Vol. 94, pp. 337-345, 1990.

26. Ott, S., P. Schurtenberger and H. Wunderli-Allenspach, "Liposomes and Influenza Viruses as an in vitro Model for Membrane Interactions II. Influence of Vesicle size and Preparation Methods", *European J. of Pharmaceutical Sci*., Vol.1, pp. 333-341, 1994.

27. Petkoval, V., M. Nedyalkov and J. J. Benattar, "Freestanding Black Films of Phospholipids and Phospholipid Proteins", *Colloids and Surfaces A: Physicochem. Eng. Aspects*, Vol. 190, pp. 9-16, 2001.

28. McDonald, R. C., R. L. McDonald, B. Ph. M. Menco, K. Takeshita, N. K. Subbarao and L. Hu, "Small-Volume Extrusion Apparatus for Preparation of Large, Unilamellar Vesicles", *Biochim. Biophys*., Vol. 106, pp.297-303, 1991.

29. Gradzielski, M., "Investigations of the Dynamics of Morphological Transitions in Amphiphilic Systems", *Current Opinion in Colloid and Interface Science*, Vol. 9, pp. 256-263, 2004.

30. Bossev, D. P. and N. S. Rosov, "*Biomembrane Flexibility Studied in the Presence of Cholesterol and Salt*", http://www.ncnr.nist.gov/AnnualReport/FY2003_html/RH7, 2003.

31. Zhang, X., A. B. Patel, R. A. de Graaf and K. L. Behar, "Determination of Liposomal encapsulation Efficiency Using Proton NMR Spectroscopy", *Chemistry and Physics of Lipids*, Vol. 127, pp.113-120, 2004.

32. Dahim, M., J. Gustafsson, F. Puisieux and M. Ollivon, "Solubilization of Phospholipid/Triacylglycerol Aggregates by Non-Ionic Surfactants", *Chemistry and Physics of Lipids*, Vol. 97, pp.1-14, 1998.

33. Robinson, B. H., S. Bucak and A. Fontana, "On the Concept of Driving Force Applied to Micelle and Vesicle Self-Assebly", *Langmuir*, Vol. 16, pp. 8231-8237, 2000.

34. Bucak, S., B. H. Robinson and A. Fontana, "Kinetics of Induced Vesicle Breakdown for Cationic and Catanionic Systems", *Langmuir*, Vol. 18, pp. 8288-8294, 2002.

35. Beugin, S., K. Edwards, G. Karlsson, M. Ollivon and S. Lesiur, "New Sterically Stabilized Vesicles Based on Nonionic Surfactant, Cholesterol, and Poly(Ethylene Glycol)-Cholesterol Conjugates",*Biphyical Journal*, Vol. 74, pp. 3198- 3210, 1998.

36. McKelvey, C. A., E. W. Kaler, J. A. Zasadzinski, B. Coldren and H. T. Jung, "Templating Hollow Polymeric Spheres form Catanionic Equilibrium Vesicles: Synthesis and Characterization", *Langmuir*, Vol. 16, pp. 8285-8290, 2000.

37. Hantz E., A. Cao and E. Taillandier, "Effect of ethanol on dimyristoylphosphatidylcholine large unilamellar vesicles investigated by quasi-elastic light scattering and vibrational spectroscopy", *Chem. Phys. Lipids*, Vol. 49, Iss. 3, pp.143-151, 1988.

38. Hallett F. R., B. Nickel, C. Samuels and P. H. Krygsman, "Determination of Vesicle Size Distributions by Freeze-Fracture Electron Microscopy", *J. Electron Microsc. Tech.*, Vol. 17, Iss. 4, pp. 459-66, 1991.